NUMERICAL INVESTIGATION ON CONVECTIVE HEAT TRANSFER ENHANCEMENT USING VARIOUS NANO FLUIDS AND DIFFERENT DUCT GEOMETRIES

PRESENTED BY:

Sai Praneeth 711956

Srikar 711928

Sai Ganesh 711919

Yuvaraj 711961

SUPERVISOR

Dr. Santhosh kumar

MECHANICAL DEPARTMENT

NATIONAL INSTITUTE OF TECHNOLOGY

ANDHRA PRADESH -534102, INDIA.

Contents

Contents

Introduction

- Fossil fuels are non-renewable sources of energy extracted from dead plants and animals.
- They cause environmental pollution, contribute to climate change, and have finite reserves and major contributors to air and water pollution.
- Extraction and transportation can cause environmental disasters, and dependence on them can cause economic vulnerability.
- Burning fossil fuels emits greenhouse gases and contributes to global warming.
- Solar water heaters use sunlight to heat water for domestic or industrial use.
- They are cost-effective, environmentally friendly, and reduce dependence on fossil fuels.
- Solar water heaters use sunlight to heat water for domestic or industrial use.

Introduction

- They are cost-effective, environmentally friendly, and reduce dependence on fossil fuels.
- Solar water heaters require minimal maintenance and emit no greenhouse gases.
- They can be installed in homes, hotels, hospitals, and other buildings to provide hot water.
- Infusing pure water with nanoparticles can significantly improve the convective heat transfer efficiency of solar water heaters.
- This technique involves adding tiny metal or metal oxide particles to the water to enhance its thermal conductivity, allowing it to absorb and transfer heat more efficiently.
- **In our project we are analysing the effect of using SiO_2 TiO_2 and Al_2O_3 based nanofluids in improving the convective heat transfer of solar water heater.**

Applications:

- Heat Exchangers.(Heat exchangers are used more often to dissipate heat)
- Laser cooling
- Cooling techniques
- Thermal reservoirs
- Usage of Boilers

Literature Review:

Authors	Flow passage	Type of Nanofluid	Outcomes
Ferrouillat, S., Bontemps, A., Ribeiro, J. P., Gruss, J. A., & Soriano, O. (2011)	circular tube	CuO/water nanofluid	Both theoretical and experimental results indicate that heat-transfer coefficients increase with nanoparticle concentration as well as the Peclet number.
Mohammed, H. A., Om, N. I., Shuaib, N. H., Hussein, A. K., & Saidur, R. (2011).	Equilateral triangular duct	Au , SiO2/water nanofluid	. It is found that SiO 2 nanofluid has the highest Nusselt number while Au nanofluid has the lowest Nusselt number among other nanofluids. The apex angle of the triangular duct has remarkable influence on the Nusselt number. An increasing of the duct apex angle decreases the Nusselt number value.
Hanks, R. W., & Cope, R. C. (1970).	isosceles triangular cross section	water	for the case of steady, isothermal, fully developed flow of Newtonian fluids in straight ducts of constant isosceles triangular cross section., the simultaneous existence of macroscopically large stable regions of laminar and turbulent flow are predicted to occur during the transition phenomenon.

Literature Review:

Authors	Flow passage	Working fluid	Outcomes
Aggarwala, B. D., & Gangal, M. K. (1975)	equilateral and right isosceles triangles	CuO/water nanofluid	solving an integro-differential eigenvalue problem arising in the discussion of laminar flow development in ducts. Application is made to equilateral and right isosceles triangles..
Ali, M. E., & Al-Ansary, H. (2009, January)	vertical triangular cross section	air	Axial (perimeter averaged) heat transfer coefficients along the side of each duct are obtained for laminar and transition to turbulent regimes of natural convection heat transfer. Axial (perimeter averaged) Nusselt numbers are evaluated and correlated using the modified Rayleigh numbers for laminar
Xuan, Y., & Li, Q. (2000).	Circular tube	Transformer oil + Cu nanoparticles suspenion Water+Cu nanoparticles	he hot-wire method has been used tomeasure the thermal conductivity of nanoØuids..

Literature Review:

Authors	Flow passage	Working fluid	Outcomes
Alawi, O. A., Sidik, N. A. C., Mohammed, H. A., & Syahrullail, S. (2014)	-	Al203, Au and SiO2 based nano fluids	The exercise's main objective was to compare thermal conductivity data obtained by different organizations for the same samples. Four sets of test nanofluids were procured
Khanafer, K., & Vafai, K. (2011)	vertical triangular cross section	Al_2O_3/water nanofluid	. Correlations for effective thermal conductivity and viscosity are synthesized and developed in this study in terms of pertinent physical parameters based on the reported experimental data.
Zhou, S. Q., & Ni, R. (2008).	Circular tube	Al_2O_3/water nanofluid	presented an experimental investigation of the specific heat c of the water-based Al2O3 nanofluid with DSC measurement. It has been found that the specific heat of nanofluid decreases with increasing nanoparticle volume fraction and their relationship is in with the prediction of the thermal equilibrium model [

Literature Review:

Authors	Flow passage	Working fluid	Outcomes
Aggarwala, B. D., & Gangal, M. K. (1975)	equilateral and right isosceles triangles	CuO/water nanofluid	solving an integro-differential eigenvalue problem arising in the discussion of laminar flow development in ducts. Application is made to equilateral and right isosceles triangles..
Ali, M. E., & Al-Ansary, H. (2009, January)	vertical triangular cross section	air	Axial (perimeter averaged) heat transfer coefficients along the side of each duct are obtained for laminar and transition to turbulent regimes of natural convection heat transfer. Axial (perimeter averaged) Nusselt numbers are evaluated and correlated using the modified Rayleigh numbers for laminar
Xuan, Y., & Li, Q. (2000).	Circular tube	Al_2O_3/water nanofluid	he hot-wire method has been used tomeasure the thermal conductivity of nanofuids..

Literature Review:

Authors	Flow passage	Type of Nanofluid	Outcomes
Heris, S. Z., Esfahany, M. N., & Etemad, G. (2006).	circular tube	CuO/water nanofluid	Both theoretical and experimental results indicate that heat-transfer coefficients increase with nanoparticle concentration as well as the Peclet number.
Edalati, Z., Zeinali Heris, S., & Noie, S. H. (2012)	Equilateral triangular duct	CuO/water nanofluid	The heat transfer increases with the nanofluid volume concentration as well as the Peclet number, a 41% enhancement in the convective heat transfer coefficient for a 0.8% CuO/water nanofluid can be seen when compared to pure water.
Manca, O., Nardini, S., Ricci, D., & Tamburrino, S. (2012)	Equilateral triangular duct	Al_2O_3/water nanofluid	There is a increase of average convective heat transfer coefficient and Nusselt number for increasing values of Richardson number and particle concentration, also wall shear stress and required pumping power profiles grow significantly.

Literature Review:

Authors	Flow passage	Type of Nanofluid	Outcomes
Mansour, R. B., Galanis, N., & Nguyen, C. T. (2011).	Inclined copper tube	Al_2O_3/water nanofluid	They developed correlations to calculate the Nusselt number in fully developed region for horizontal and vertical tubes. a higher particle volume concentration induces a decrease of the Nusselt number for the horizontal inclination. On the other hand, for the vertical one, the Nusselt number remains nearly constant with an increase of particle volume concentration from 0 to 4%.
Heris, S. Z., Edalati, Z., Noie, S. H., & Mahian, O. (2014).	Equilateral triangular duct	Al_2O_3/water nanofluid	The heat transfer enhancement increases with increases in the nanofluid volume concentration and Peclet number.

Gap Analysis

Peng et al. (2017) investigated the convective heat transfer of Al2O3-water nanofluids in a flat plate solar collector. They found that the heat transfer coefficient was enhanced by up to 28% for the nanofluid compared to pure water, and that the enhancement increased with increasing nanoparticle concentration.

We concluded the same for 3 different nano fluids (SiO_2 TiO_2 and Al_2O_3) and obtain highest heat transfer for Al_2O_3 based nano fluid

Our work concluded that using equilateral triangular cross sectioned duct increased 14.96% in HTC and upto 70.34 % increase when using an trapezoidal duct with inner angle 80 degrees compared to pure fluid.

Gap Analysis

Equilateral triangular duct with Al2O3/water nanofluid: There is an increase in the average convective heat transfer coefficient and Nusselt number for increasing values of Richardson number and particle concentration. (Manca et al., 2012 and Heris et al., 2014)

Our work concluded that using equilateral triangular cross sectioned duct increased 14.96% in HTC and upto 70.34 % increase when using an trapezoidal duct with inner angle 80 degrees compared to pure fluid.

Objectives

- Observing how thermo-physical and thermal properties of nanofluids are varying with volume concentrations.
- Comparing different nanofluids for enhanced heat transfer.
- Inferencing the convective heat transfer at different locations within the duct from the fluid streamlines.
- Evaluating maximum heat transfer properties for different duct geometries.

Problem Description

- In our present work , a comparison is done for different nano fluids (SiO_2 TiO_2 and Al_2O_3) to understand their convective heat transfer performance for volume concentrations varying from 0% – 4% and at Richardson's numbers = { 0.1 , 0.5 , 1 , 2 , 3 , 5}
- We considered an equilateral triangular duct with side length of 17mm and duct length 2 metre.
- A Uniform Heat flux is applied to all three rectangular sides of the triangular cross sectioned duct.
- We also consider six other geometries with one rectangular duct , 4 isosceles trapezoidal ducts with base angles of 50 deg, 60 deg, 70 deg & 80 deg and isosceles triangle of 45 deg.

Methodology:

- The study has been done on steady state and fully developed regime flow.
- The numerical analysis on three dimensional triangular duct model is solved by computational fluid dynamic(CFC) code “Ansys Fluent 18.1” for varying volume concentrations, varying Richardson numbers and for different nanofluids.
- The flow is steady state, incompressible, laminar flow with constant temperature and we assumed Boussinesq approximation.
- The single-phase model approach is employed for nanofluids. A second-order upward scheme is employed for energy and momentum equations.

Methodology:

- The ‘SIMPLE’ coupling scheme was employed to couple pressure and velocity.
- A convergence criteria of 10^(-4), 10^(-5)and 10^(-8) were assumed for the residuals of continuity, velocity components and energy respectively.
- No-slip condition was applied on duct walls, and temperature and density variations are ignored along the duct.

Numerical Methodology:

- The governing equations of continuity, momentum and energy equations in 3-D form were solved by means of FLUENT code.

$$\frac{\partial u}{\partial x}+\frac{\partial v}{\partial y}+\frac{\partial w}{\partial z}=0$$

Continuity Equation

$$u\frac{\partial u}{\partial x}+v\frac{\partial u}{\partial y}+w\frac{\partial u}{\partial z}+\frac{1}{\rho}\frac{\partial P}{\partial x}=\upsilon\left(\frac{\partial^2 u}{\partial x}+\frac{\partial^2 u}{\partial y^2}+\frac{\partial^2 u}{\partial z^2}\right)$$

$$u\frac{\partial v}{\partial x}+v\frac{\partial v}{\partial y}+w\frac{\partial v}{\partial z}+\frac{1}{\rho}\frac{\partial P}{\partial y}=\upsilon\left(\frac{\partial^2 v}{\partial x}+\frac{\partial^2 v}{\partial y^2}+\frac{\partial^2 v}{\partial z^2}\right)$$

$$u\frac{\partial w}{\partial x}+v\frac{\partial w}{\partial y}+w\frac{\partial w}{\partial z}+\frac{1}{\rho}\frac{\partial P}{\partial z}=\upsilon\left(\frac{\partial^2 w}{\partial x}+\frac{\partial^2 w}{\partial y^2}+\frac{\partial^2 w}{\partial z^2}\right)$$

Momentum Equation

$$u\frac{\partial T}{\partial x}+v\frac{\partial T}{\partial y}+w\frac{\partial T}{\partial z}=\alpha\left(\frac{\partial^2 T}{\partial x}+\frac{\partial^2 T}{\partial y^2}+\frac{\partial^2 T}{\partial z^2}\right)$$

Energy Equation

Geometrical description

- A three-dimensional duct with an equilateral triangular cross section is investigated as shown in figure-1.
- According to figure-1, the overall length L is 2.0 m, whereas the internal edge l is 0.017m.The hydraulic diameter, dh = 4A/Ph, is therefore equal to 0.01 m.

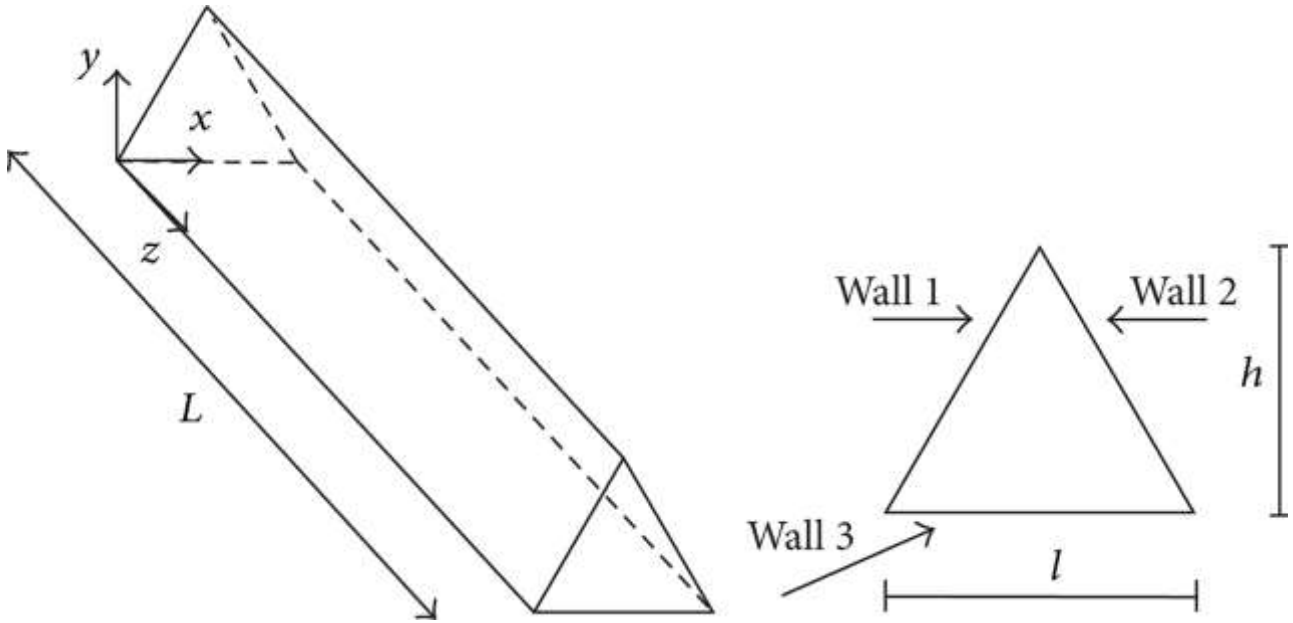

Figure-1: Equilateral triangular duct and its cross-sectional view

Boundary Conditions:

The assigned boundary conditions for the study are as follows:

- Inlet Section: The inlet section is assigned a uniform velocity and temperature profile to maintain a steady flow throughout the duct. The velocity profile is set to a constant value, and the temperature profile is also set to a constant value to ensure that the flow remains isothermal.

- Outlet Section: The outlet section is assigned an outflow condition where the velocity components and temperature derivatives are equal to zero. This condition ensures that the fluid exits the duct without any disturbance and that the flow remains steady-state.

Boundary Conditions:

- Duct Surfaces: The duct surfaces are assigned a no-slip condition, where the velocity components are equal to zero. This condition ensures that the fluid sticks to the surface of the duct and doesn't slip past it. The duct surfaces are also assigned a uniform heat flux to maintain a constant temperature throughout the duct. This condition ensures that there is a continuous transfer of heat between the fluid and the duct surfaces.

- These boundary conditions ensure that the flow remains steady-state, isothermal, and that there is a continuous transfer of heat between the fluid and the duct surfaces. The Boussinesq approximation ensures that the buoyancy effects are taken into account, which is important for accurately analysing the convective heat transfer performance of the nanofluids

Meshing

- Meshing is one of the most important steps in performing an accurate simulation using FEA. A mesh is made up of elements which contain nodes (coordinate locations in space that can vary by element type) that represent the shape of the geometry.
- Any continuous object has infinite degrees of freedom (DOF) which makes it impossible to solve using hand calculations. So in FVM, we create a mesh which splits the domain into a discrete number of elements for which the solution can be calculated.

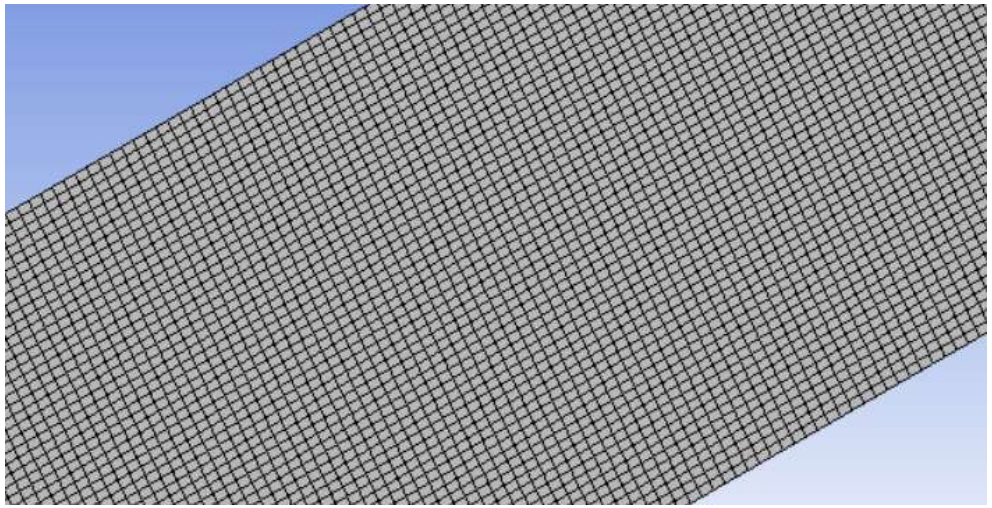

Figure-2: Meshed figure of Triangular Duct

Grid Independent Analysis:

- The grid independence test is a process used to find the optimal grid condition that has the smallest number of grids without generating a difference in the numerical results based on the evaluation of various grid conditions.
- We had used 31840, 60000, 111300, 341829, 757614, 1024458, 2296574 nodes for 22260, 44955, 87384, 287712, 662000, 903279, 2088000 number of elements, respectively to accomplish grid-sensitivity test.
- The respective Nusselt numbers and mesh size is mentioned in table-1.
- To accomplish a optimal solution we used 1521856 elements and 1716900 nodes with a mesh size of 0.45 mm.

Grid Independent Analysis:

S.NO	Number of Elements	Nusselt Number
1	10697	0.091891039
2	23744	0.09209474
3	37925	0.091572295
4	95944	0.091290553
5	177413	0.091204188
6	245735	0.091215578
7	424072	0.09125459
8	2036320	0.091257739
9	2323456	0.091257801

Table-1: Nusselt Numbers for different Mesh size taken at 0% volume concentration and Richardson number equal to 0.1

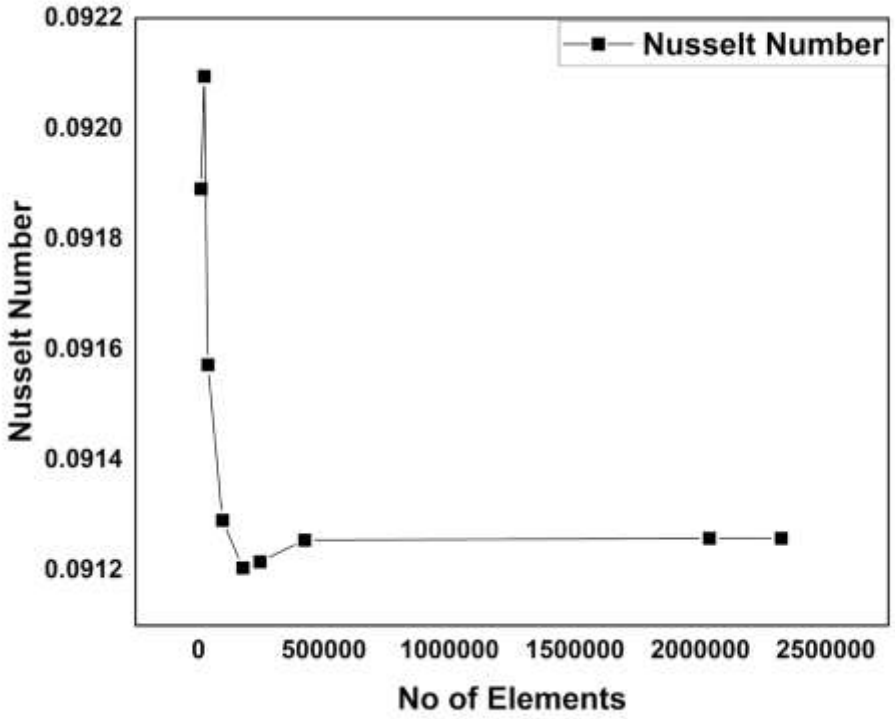

Graph-1: Nusselt number vs No of Elements

Validation:

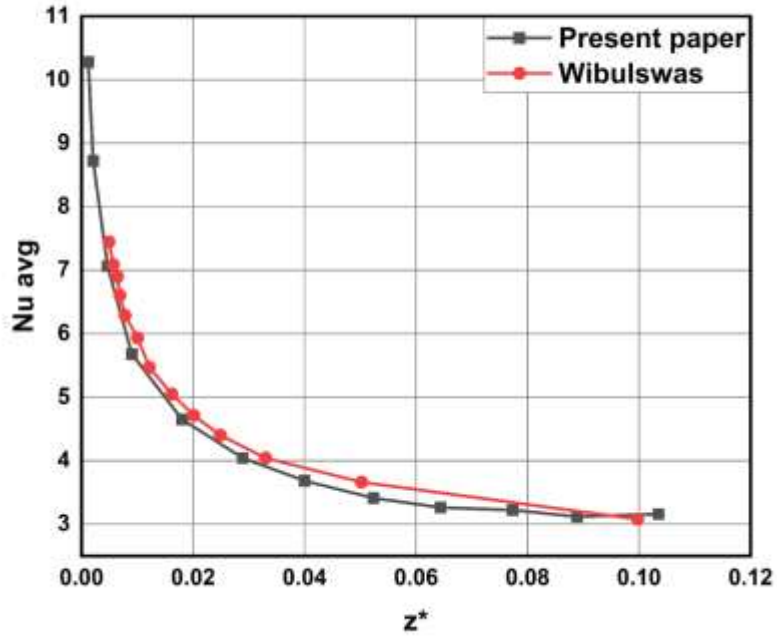

Graph-2: Validation of average Nusselt Number

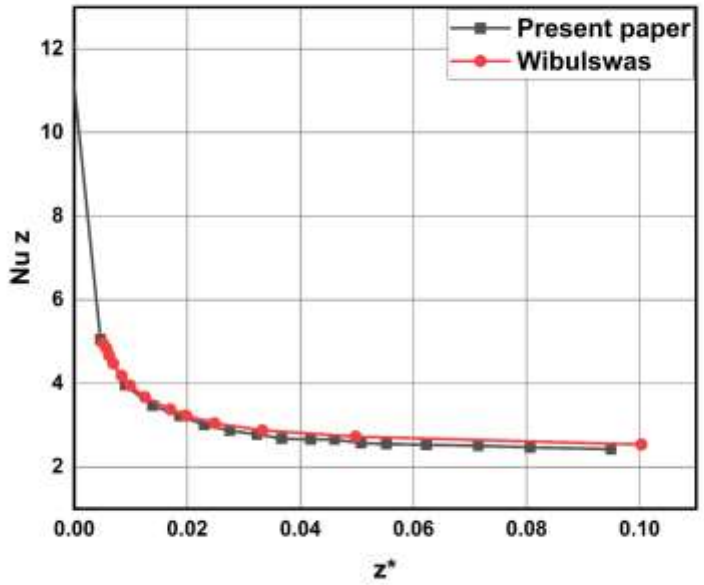

Graph-3: Validation of Local Nusselt Number

Data Reduction:

- The dimensionless parameters of Reynolds number, Grashof number, Richardson number, Nusselt number and friction factor are considered for the data reduction and they are expressed by the following relations:

$$\mathrm{Re} = \frac{V d_h}{\nu},$$

$$\mathrm{Gr} = \frac{g\beta \dot{q} {d_h}^4}{\lambda \nu^2},$$

$$\mathrm{Ri} = \frac{\mathrm{Gr}}{\mathrm{Re}^2},$$

$$\mathrm{Nu_{av}} = \frac{\dot{q} d_h}{(T_w - T_m)\lambda_f},$$

$$f = 2\Delta P \frac{d_h}{L} \frac{1}{\rho V^2},$$

Where V is average inlet velocity, q is heat flux, Tw and Tm represents the average surface temperature and bulk fluid temperature, respectively

Material Properties of Particles:

- Here we are using three nanoparticles infused in base fluid water, those are Aluminum oxide, titanium oxide and silicon oxide. There respective material properties are shown below:

	Density[kg/m3]	Specific Heat[J/Kg.K]	Volumetric Expansion Coefficient[1/K]	Dynamic Viscosity[Pa.s]	Thermal conductivity[W/m.K]
Al_2O_3	3880	773	//	//	36
Water	998.2	4182	2.10e-4	993e-6	Material0.597

Table-2: Aluminum oxide Material properties at T=293 K.

Material Properties of Particles:

Material	Density[kg/m3]	Specific Heat[J/Kg.K]	Volumetric Expansion Coefficient[1/K]	Dynamic Viscosity[Pa.s]	Thermal conductivity[W/m.K]
TiO_2	4250	686.2	2.6e-8	//	8.9
Water	998.2	4182	2.10e-4	993e-6	0.597

Table-3: Titanium oxide Material properties at T=293 K.

Material	Density[kg/m3]	Specific Heat[J/Kg.K]	Volumetric Expansion Coefficient[1/K]	Dynamic Viscosity[Pa.s]	Thermal conductivity[W/m.K]
SiO_2	2220	745	4e-6	//	10.4
Water	998.2	4182	2.10e-4	993e-6	0.597

Table-4: Silicon oxide Material properties at T=293 K.

Correlations formulas varying by volumetric concentrations:

$$\text{Density:}\quad \rho_{nf} = (1-\phi)\,\rho_{bf} + \phi\rho_p,$$

$$\text{Specific heat:}\quad (\rho c_p)_{nf} = (1-\phi)\,(\rho c_p)_{bf} + \phi(\rho c_p)_p,$$

$$\text{Thermal expansion coefficient:}\quad \frac{\beta_{nf}}{\beta_{bf}} = \frac{1}{(((1-\phi)/\phi)(\rho_{bf}/\rho_p))}\frac{\beta_p}{\beta_{bf}} + \frac{1}{((\phi/(1-\phi))(\rho_{bf}/\rho_p)+1)}.$$

$$\text{Dynamic viscosity:}\quad \frac{\mu_{nf}}{\mu_{bf}} = \frac{1}{1-34.87(d_p/d_f)^{-0.3}\phi^{1.03}}$$

With $d_f = 0.1\left(6M/N\pi\rho_{f,0}\right)$ in which M is the molecular weight of the base fluid, N is the Avogadro number, and $\rho_{f,0}$ is the mass density of the base fluid calculated at T = 293 K

$$\text{Thermal conductivity:}\quad \frac{\lambda_{nf}}{\lambda_{bf}} = 1 + 4.4\mathrm{Re}^{0.4}\mathrm{Pr}^{0.66}\left(\frac{T}{T_{fr}}\right)^{10}\cdot\left(\frac{\lambda_p}{\lambda_{bf}}\right)^{0.03}\phi^{0.66}$$

Thermo-Physical Properties of Nanofluids:

- Here we are using water based Aluminum oxide, Titanium oxide and Silicon oxide nanofluids. There respective Thermo-Physical properties are shown below:

Volume concentration	Density[kg/m3]	Specific Heat[J/Kg.K]	Volumetric Expansion Coefficient[1/K]	Dynamic Viscosity[Pa.s]	Thermal conductivity[W/m.K]
0%	998.2	4182	2.1e-4	993e-6	0.597
1%	1027	4053	2.098e-4	1082e-6	0.622
2%	1056	3931	2.095e-4	1193e-6	0.636
4%	1113	3707	2.09e-4	1511e-6	0.658

Table-5: Water based Aluminum oxide Nanofluid Thermo-physical properties at T=293 K.

Volume concentration	Density[kg/m3]	Specific Heat[J/Kg.K]	Volumetric Expansion Coefficient[1/K]	Dynamic Viscosity[Pa.s]	Thermal conductivity[W/m.K]
0%	998.2	4182	2.1e-4	993e-6	0.597
1%	1030.718	4037.85631	2.095e-4	1035.68e-6	0.59847
2%	1063.236	3902.5296	2.09e-4	1084.24e-6	0.59932
4%	1128.272	3655.2772	2.0798e-4	1199.06e-6	0.60067

Table-6: Water based Titanium oxide Nanofluid Thermo-physical properties at T=293 K.

Volume concentration	Density[kg/m3]	Specific Heat[J/Kg.K]	Volumetric Expansion Coefficient[1/K]	Dynamic Viscosity[Pa.s]	Thermal conductivity[W/m.K]
0%	998.2	4182	2.1e-4	993e-6	0.597
1%	1010.418	4106.48532	2.0914e-4	1018.47e-6	0.600717
2%	1022.636	4032.77505	2.0827e-4	1045.23e-6	0.60287
4%	1047.072	3890.51517	2.0650e-4	1102.62e-6	0.60628

Table-7: Water based Silicon oxide Nanofluid Thermo-physical properties at T=293 K.

Results and Discussion:

- Results are obtained for 3 different nanofluids and we considered Reynolds number as constant value 100, Richardson number varying as 0.1, 0.5, 1, 2, 3, 5, and 0%, 1%, 2%, 4% volume concentrations.
- Results are reported in terms of average convective heat transfer coefficient, average Nusselt number, wall shear stress and required pumping power profiles.
- The above result profiles are considered for varying volume concentrations and for 3 different nanofluids.

Various profiles for Water based Aluminum-oxide Nanofluid

Heat Transfer Coefficient for different Richardson numbers and different volume concentration values:

- HTC increases with increase in volume concentration of nanoparticles.
- HTC for different Richardson's number ranges from 5.448133 to 108.3699.
- The percentage increase of HTC at 1%,2%,4% with respective to the HTC at 0% is calculated by:

  % Change = (HTC **at x% - **HTC **at 0%) /** HTC **at 0%**
- For Richardson number 0.1:
  % change for 1% = 2.37% for 2% = 5.50% for 4% = 14.96%
- For Richardson number 2:
  % change for 1%= 1.51% for 2% = 3.59% for 4%: 9.63%
- For Richardson number 5:
  % change for 1% = 1.21 for 2% = 2.84% for 4%: 7.79%
- As Richardson number is increasing HTC increases and after a certain Richardson number it is becoming constant.

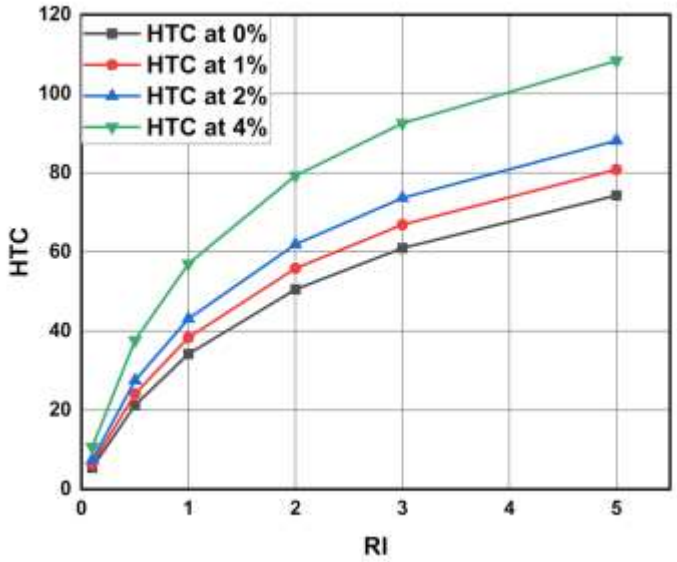

Graph-4: Richardson number vs average heat transfer coefficient values for different volume concentrations.

Nusselt Numbers for different Richardson numbers and different volume concentration values:

- Nusselt number increases with increase in volume concentration.
- Nu value for different Richardson's number ranges from 0.09126 to 1.64696
- The percentage increase of Nusselt number at 1%,2%,4% with respective to the Nusselt number at 0% is calculated by

  % Change = (Nu at x% - Nu at 0%) / Nu at 0%
- For Richardson number = 0.1:
  % Change at 1% = 11.22% % , 2% = 29.54% , 4% = 77.68%
- For Richardson number = 2:
  % Change at 1% = 6.11% , 2% = 17.65% , 4% = 42.25%
- For Richardson number = 5:
  % Change at 1% = 4.39% , 2% = 13.86% , 4% = 32.25%
- However the percentage of increase in Nusselt number decreases and becomes constant due to law of diminishing returns.
- This Implies increasing the concentration linearly doesn't increase the Nusselt number linearly.

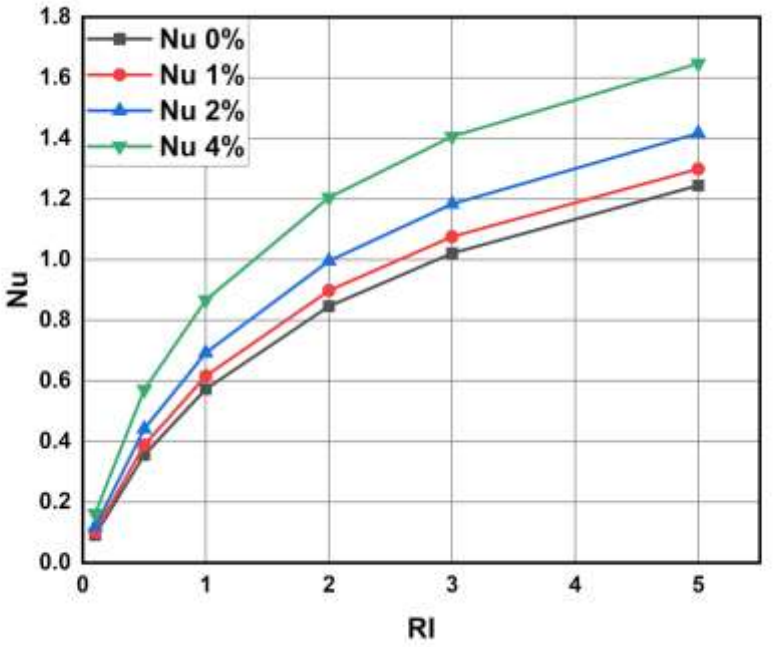

Graph-5: Richardson Number vs Nusselt Number values for different volume concentrations.

Average Shear stresses for different Richardson numbers and different volume concentration values:

- As Nusselt number is increasing average shear stress on walls also increasing.
- Average shear stress for different Richardson's number ranging from 0.0066354363 to 0.01694618
- The percentage change in avg shear stress compared with 0% concentration as reference are as follows

  % Change = (value at x% - value at 0%) / value at 0%
- Richardson number 0.1:

  % change for 1%: 15.221% for 2%: 34.783% for 4%: 102.25%
- Richardson number 2:

  % change for 1%: 18.346% for 2%: 32.202% for 4%: 94.158%
- Richardson number 5:

  % change for 1%: 25.296% for 2%: 32.576% for 4%: 92.777%
- Here as concentration of nanoparticles is increasing stress are becoming 1.2 times of stress seen in pure water.

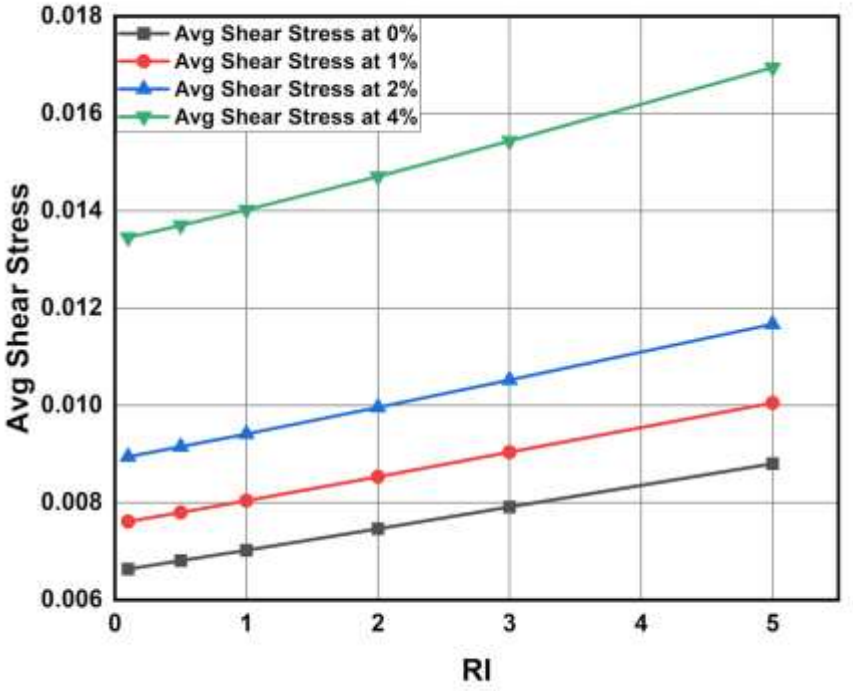

Graph-6: Richardson Number vs average Shear Stress values for different volume concentrations.

Heat Transfer Coefficient in wall-2 & wall-3 for different Richardson numbers and different volume concentration values:

- Here for wall 1 it slightly higher heat transfer coefficient values compared to that wall-2 and wall-3. This is because of gravity and weight of fluid is acting on wall-1. For wall-2 and wall-3 we are observing a almost same HTC values

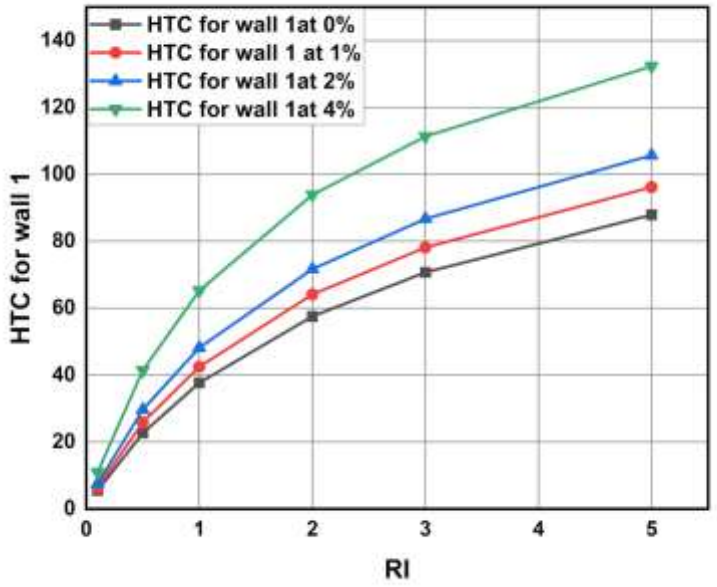

Graph-7: Richardson Number vs Heat transfer coefficient values in wall-1 avg for different volume concentrations.

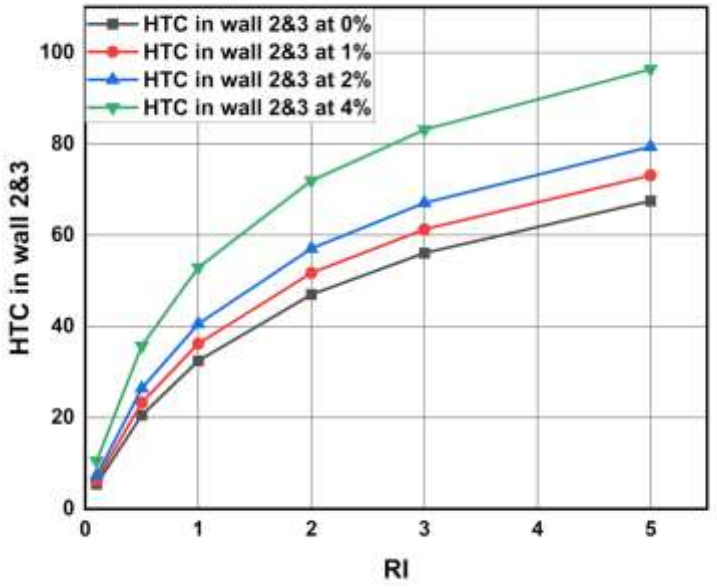

Graph-8: Richardson Number vs Heat transfer coefficient values in wall-2 ,3 avg for different volume concentrations.

Pumping Power for different Richardson numbers and different volume concentration values:

- Here as Heat transfer is increasing power required to pump the fluid into duct also increasing.
- Pumping power is increasing linearly with respective to Richardson's number.
- We calculate the percentage change with 0 % as reference
  % Change = (value at x% - value **at 0%) /** value **at 0%**
- For Richardson Number = 0.1:
  % change at 1% = 21.92% at 2% = 54.176% 4% = 180.57%
- For Richardson Number = 2:
  % change at 1% = 27.87% at 2% = 61.16% at 4% = 192.81%
- For Richardson Number = 5:
  % change at 1% = 21.60% at 2% = 52.80% at 4% = 173.04%
- At higher concentrations and at higher Richardson's number pumping power required is becoming more.

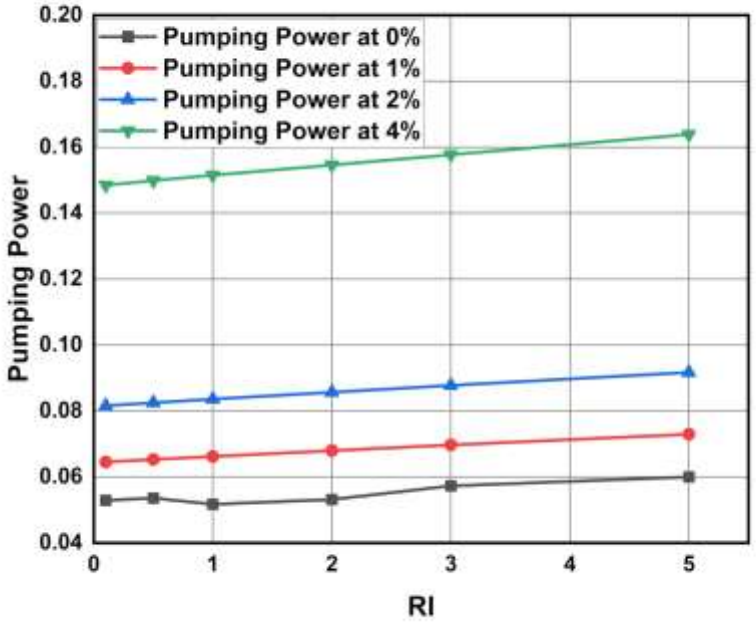

Graph-9: Richardson Number vs Pumping Power for different volume concentrations.

Various profiles for Water based Titanium-oxide Nanofluid

Heat Transfer Coefficient for different Richardson numbers and different volume concentration values:

- HTC increases with increase in volume concentration of nano particles.
- HTC for different Richardson's number ranges from 5.448133 to 80.05796
- The percentage increase of HTC at 1%,2%,4% with respective to the HTC at 0% is calculated by
  % Change = (HTC **at x% - HTC at 0%) /** HTC **at 0%**
- For Richard number 0.1:
  % change for 1% = 2.37% for 2% = 5.61% for 4% = 14.85%
- For Richard number 2:
  % change for 1%= 1.51% for 2% = 3.61% for 4%: 9.56%
- For Richard number 5:
  % change for 1% = 1.27 for 2% = 2.9% for 4%: 7.73%
- As Richardson number is increasing HTC increases and after a certain Richardson number it is becoming constant.

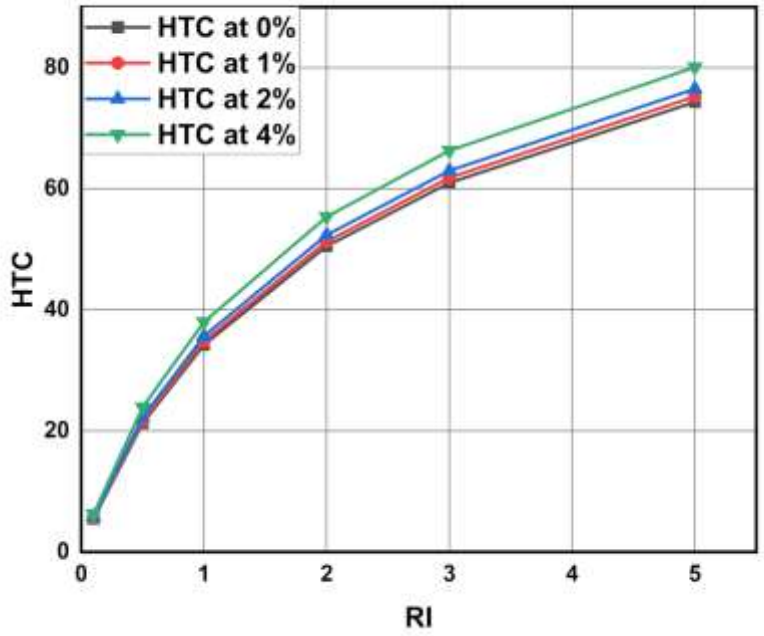

Graph-10: Richardson number vs average heat transfer coefficient values for different volume concentrations.

Nusselt Numbers for different Richardson numbers and different volume concentration values:

- Nusselt number increases with increase in volume concentration.
- Nu value for different Richardson's number ranges from 0.09126 to 1.64696
- The percentage increase of Nusselt number at 1%,2%,4% with respective to the Nusselt number at 0% is calculated by

  % Change = (Nu at x% - Nu at 0%) / Nu at 0%
- For Richardson number = 0.1:

  % Change at 1% = 2.119% % , 2% = 5.205% , 4% = 14.149%
- For Richardson number = 2:

  % Change at 1% = 1.2639% , 2% = 3.21% , 4% = 8.827%
- For Richardson number = 5:

  % Change at 1% = 0.9585% , 2% = 2.511% , 4% = 7.0794%
- However the percentage of increase in Nusselt number decreases and becomes constant due to law of diminishing returns.
- This Implies increasing the concentration linearly doesn't increase the Nusselt number linearly.

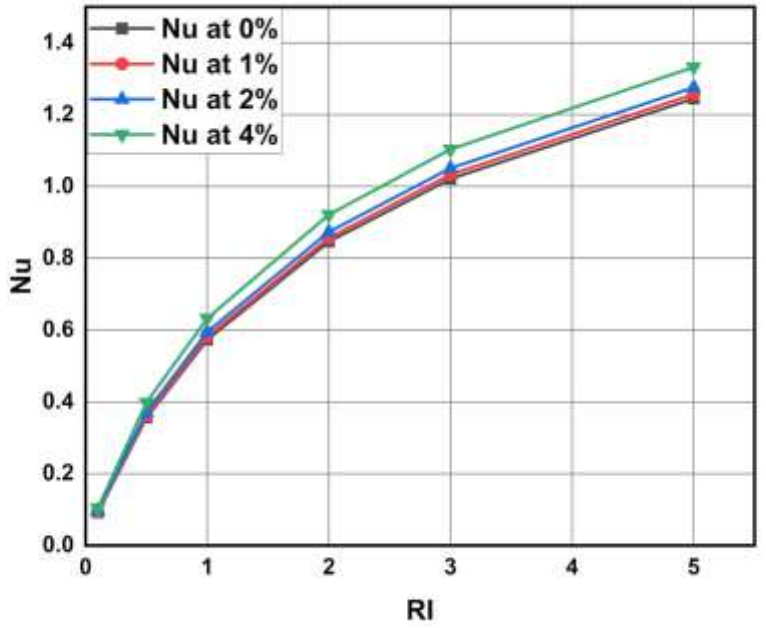

Graph-11: Richardson Number vs Nusselt Number values for different volume concentrations.

Average Shear stresses for different Richardson numbers and different volume concentration values:

- As Nusselt number is increasing average shear stress on walls also increasing.
- Average shear stress for different Richardson's number ranges from 0.0066354363 to 0.01694618
- The percentage change in Avg shear stress compared with 0% concentration as reference are as follows
- The percentage increase of Avg shear stress at 1%,2%,4% with respective to the value at 0% is calculated by

  % Change = (value at x% - value **at 0%) /** value **at 0%**
- Richardson number 0.1:

  % change for 1%: 5.2301% for 2%: 11.604% for 4%: 28.059%
- Richardson number 2:

  % change for 1%: 5.139% for 2%: 11.336% for 4%: 27.148%
- Richardson number 5:

  % change for 1%: 5.0911% for 2%: 11.16% for 4%: 26.482%

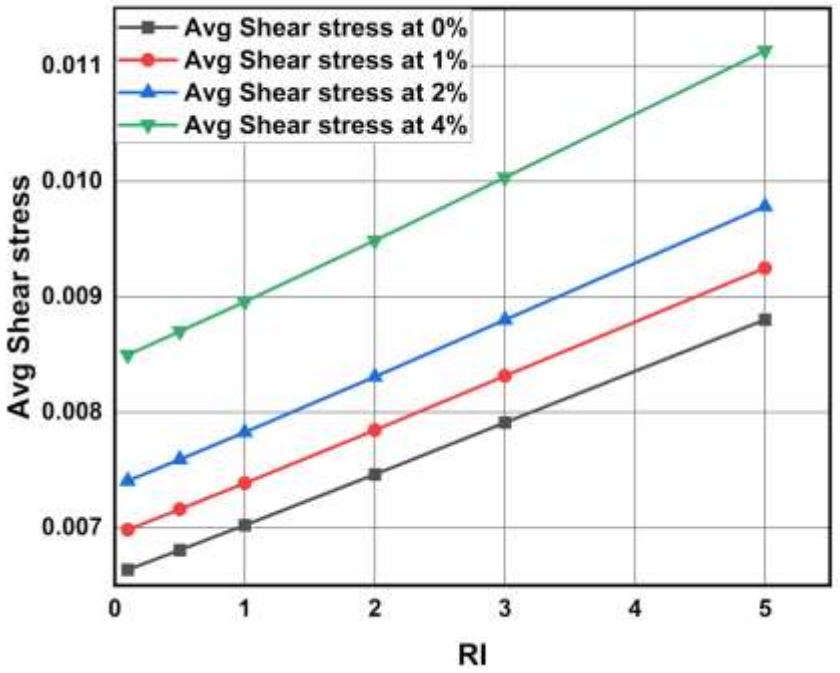

Graph-12: Richardson Number vs average Shear Stress values for different volume concentrations.

Heat Transfer Coefficient in wall-1 and wall 2&3Avg for different Richardson numbers and different volume concentration values:

- Here for wall 1 it slightly higher heat transfer coefficient values compared to that wall-2 and wall-3. This is because of gravity and weight of fluid is acting on wall-1. For wall-2 and wall-3 we are observing a same HTC values

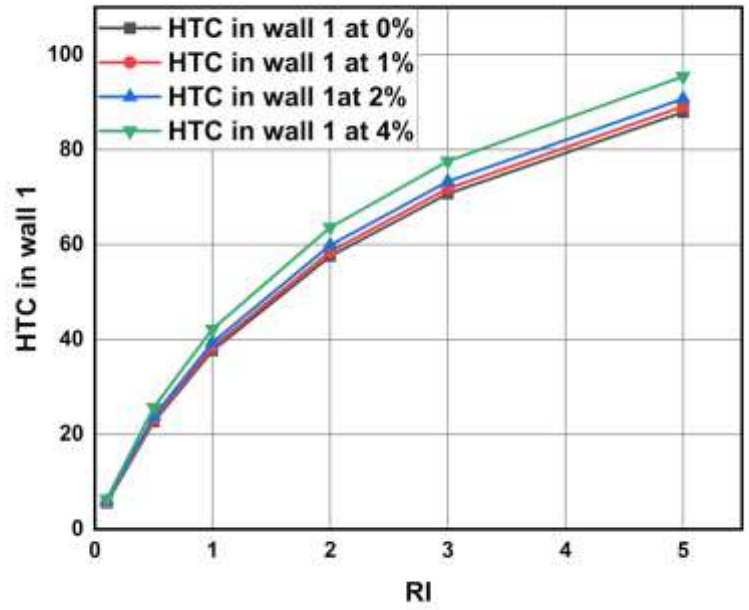

Graph-13: Richardson Number vs Heat transfer coefficient values in wall-1 for different volume concentrations.

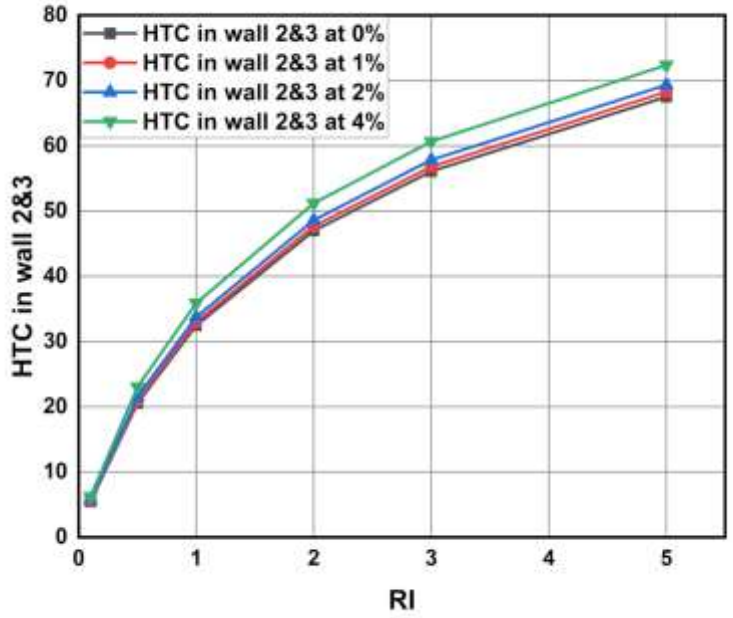

Graph-14: Richardson Number vs Heat transfer coefficient values in wall-1 for different volume concentrations.

Pumping Power for different Richardson numbers and different volume concentration values:

- Here as Heat transfer is increasing power required to pump the fluid into duct also increasing.
- Pumping power is increasing linearly with respective to Richardson's number.
- We calculate the percentage change with 0 % as reference
  % Change = (value at x% - value **at 0%) /** value **at 0%**
- For Richardson Number = 0.1:
  % change at 1% = 22.05% at 2% = 54.31% 4% =180.32%
- For Richardson Number = 2:
  % change at 1% = 27.85% at 2% = 61.23% at 4% =191.95%
- For Richardson Number = 5:
  % change at 1% = 21.55% at 2% = 52.77% at 4% = 173.03%
- At higher concentrations and at higher Richardson's number pumping power required is becoming more.

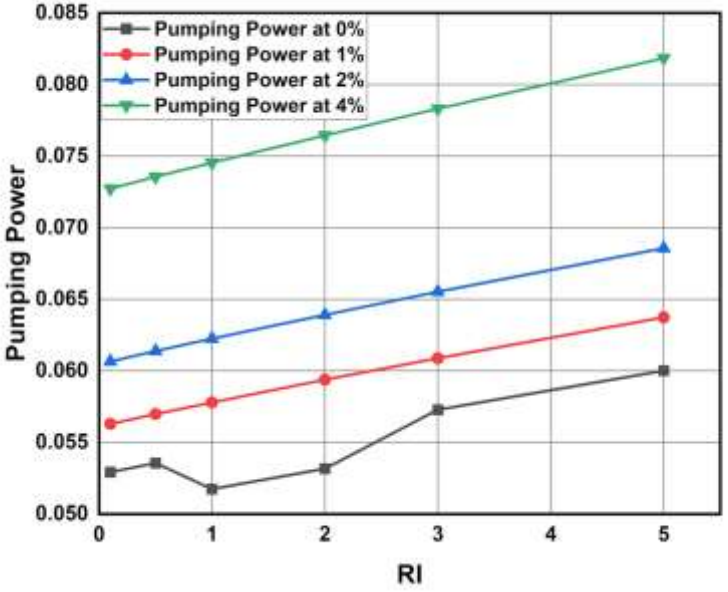

Graph-15: Richardson Number vs Pumping Power for different volume concentrations.

Various profiles for Water based Silicon-oxide Nanofluid

Heat Transfer Coefficient for different Richardson numbers and different volume concentration values:

- HTC increases with increase in volume concentration of nano particles.
- HTC for different Richardson's number ranges from 6.239 to 79.270
- The percentage increase of HTC at 1%,2%,4% with respective to the HTC at 0% is calculated by:
  % Change = (HTC **at x% -** HTC **at 0%) /** HTC **at 0%**
- For Richard number 0.1:
  % change for 1% = 3.484 % for 2% =6.96% for 4% =14.53%
- For Richard number 2:
  % change for 1%= 2.1295% for 2% = 4.217% for 4%: 8.66%
- For Richard number 5:
  % change for 1% = 1.6531 for 2% = 3.27% for 4%: 6.67%
- As Richardson number is increasing HTC increases and after a certain Richardson number it is becoming constant.

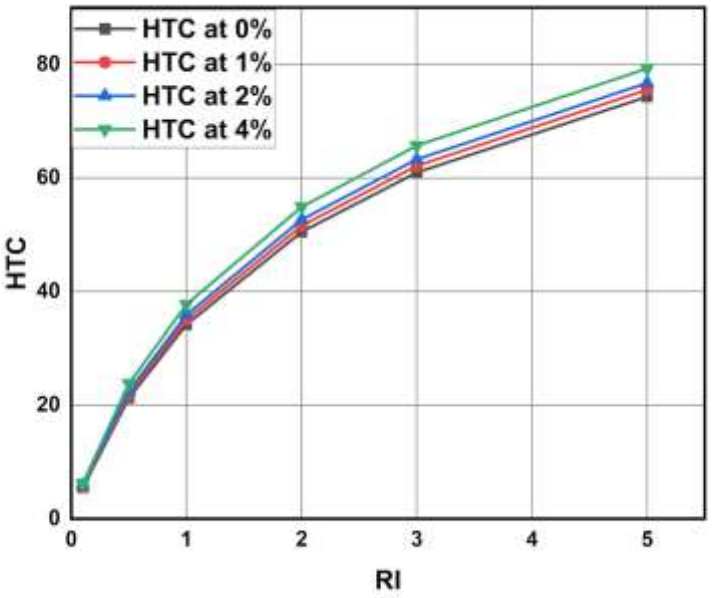

Graph-16: Richardson number vs average heat transfer coefficient values for different volume concentrations.

Nusselt Numbers for different Richardson numbers and different volume concentration values:

- Nusselt number increases with increase in concentration.
- Nu value for different Richardson's number ranges from 0.1029 to 1.307
- The percentage increase of Nusselt number at 1%,2%,4% with respective to the Nusselt number at 0% is calculated by

  % Change = (Nu at x% - Nu at 0%) / Nu at 0%
- For Richardson number = 0.1:

  % Change at 1% = 2.84% % , 2% = 5.918% , 4% = 12.77%
- For Richardson number = 2:

  % Change at 1% = 1.4976% , 2% =3.2019% , 4% = 6.9961%
- For Richardson number = 5:

  % Change at 1% =1.1241% , 2% =2.2645% , 4% = 5.0454%
- However the percentage of increase in Nusselt number decreases and becomes constant due to law of diminishing returns.
- This Implies increasing the concentration linearly doesn't increase the Nusselt number linearly

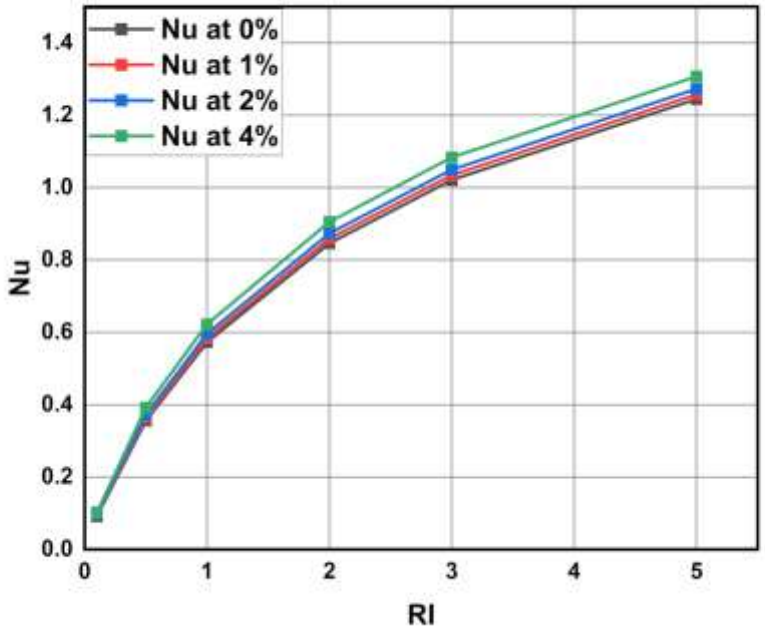

Graph-17: Richardson Number vs Nusselt Number values for different volume concentrations.

Average Shear stresses for different Richardson numbers and different volume concentration values:

- As Nusselt number is increasing average shear stress on walls also increasing.
- Average shear stress for different richardson's number ranges from 0.0066354363 to 0.01022
- The percentage change in avg shear stress compared with 0% concentration as reference are as follows

  % Change = (value at x% - value **at 0%) /** value **at 0%**

- For Richard number 0.1:
  % change for 1% = 3.7535% for 2% = 7.794% for 4% = 16.72%
- For Richard number 2:
  % change for 1%= 3.6982% for 2% = 3.59% for 4%: 16.312%
- For Richard number 5:
  % change for 1% = 3.6979 for 2% = 7.5857% for 4%: 16.182%

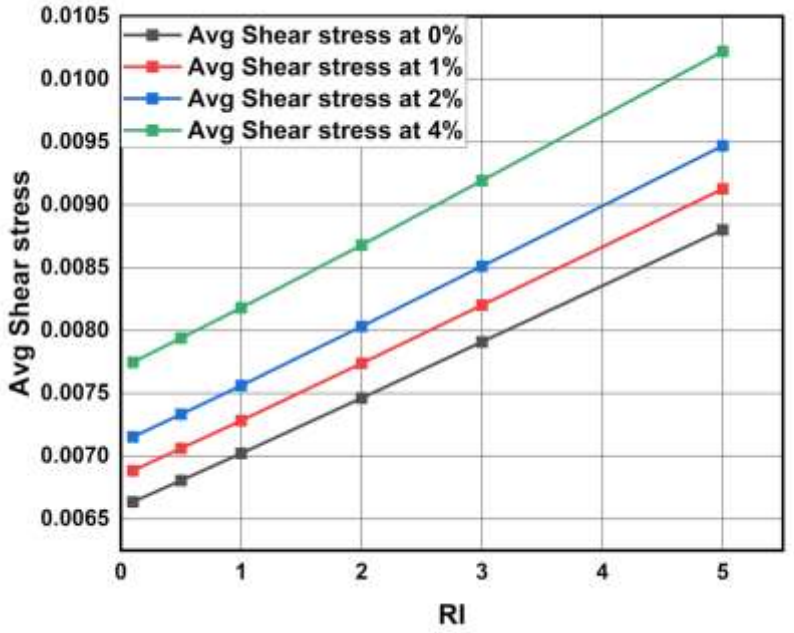

Graph-18: Richardson Number vs average Shear Stress values for different volume concentrations.

Heat Transfer Coefficient in wall-1 and wall-2&3 for different Richardson numbers and different volume concentration values:

- Here for wall 1 it slightly higher heat transfer coefficient values compared to that wall-2 and wall-3. This is because of gravity and weight of fluid is acting on wall-1. For wall-2 and wall-3 we are observing a same HTC values.

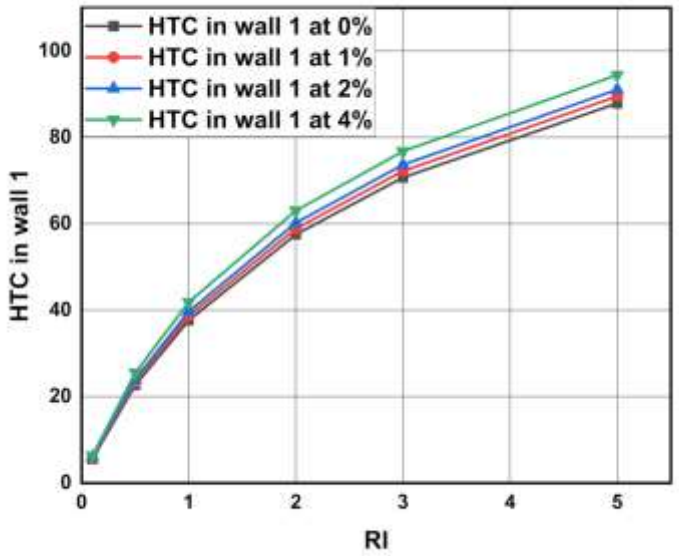

Graph-19: Richardson Number vs Heat transfer coefficient values in wall-1 for different volume concentrations.

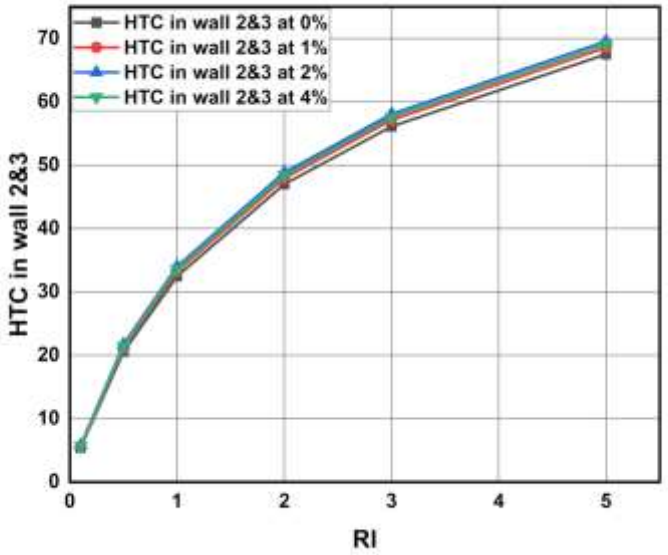

Graph-20: Richardson Number vs Heat transfer coefficient values in wall-1 for different volume concentrations.

Pumping Power for different Richardson numbers and different volume concentration values:

- Here as Heat transfer is increasing power required to pump the fluid into duct also increasing.
- Pumping power is increasing linearly with respective to Richardson's number.
- The range of pumping power is 0.0592 and 0.0852
- The percentage change with 0% concentration as reference are as follow

  % Change = (value at x% - value **at 0%) /** value **at 0%**
- For Richardson Number = 0.1:

  % change at 1% = 3.87% at 2% = 11% 4% = 42%
- For Richardson Number = 2:

  % change at 1% = 9.025% at 2% = 16.44% at 4% = 49.392%
- For Richardson Number = 5:

  % change at 1% = 3.728% at 2% = 10.76% at 4% = 41.984%
- At higher concentrations and at higher Richardson's number pumping power required is becoming more.

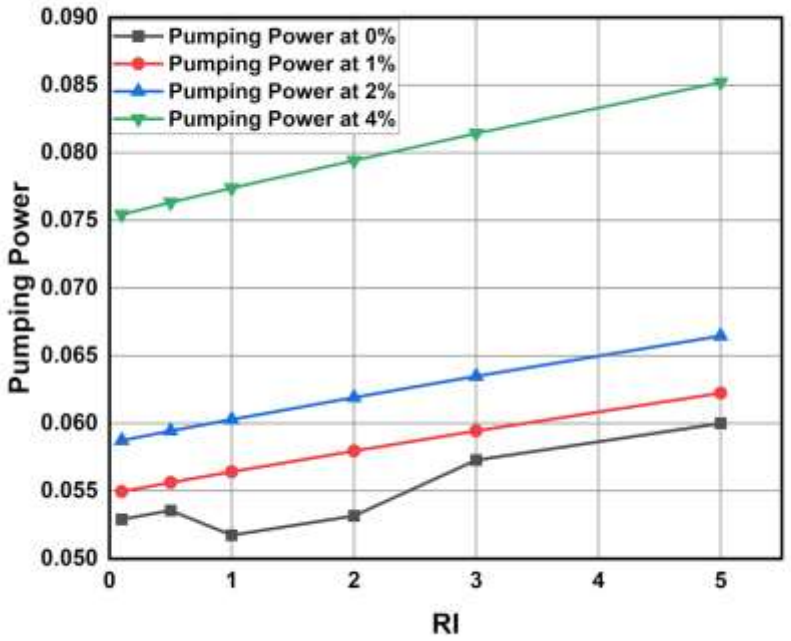

Graph-21: Richardson Number vs Pumping Power for different volume concentrations.

Comparing results between Nanofluids:

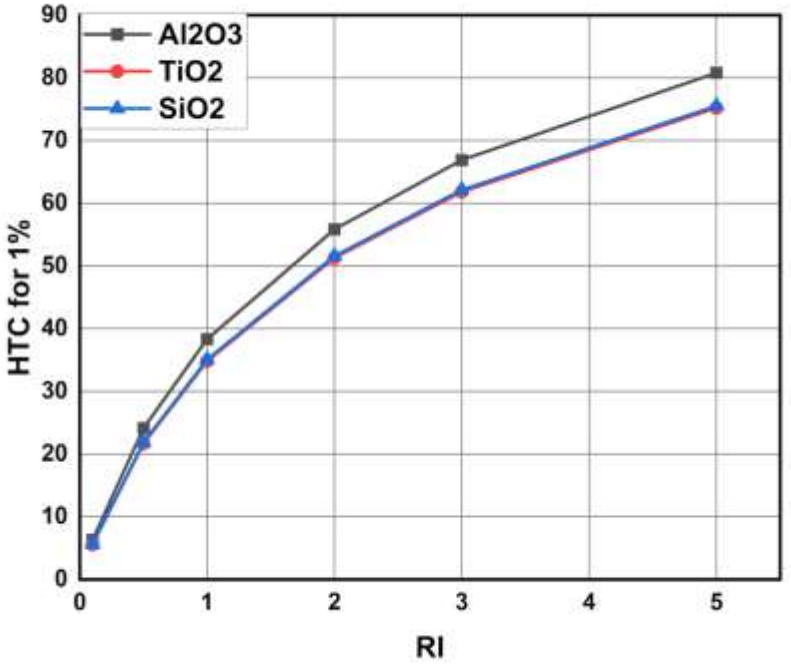

Graph-22: Heat transfer coefficient for various nanofluids at 1% volume concentration

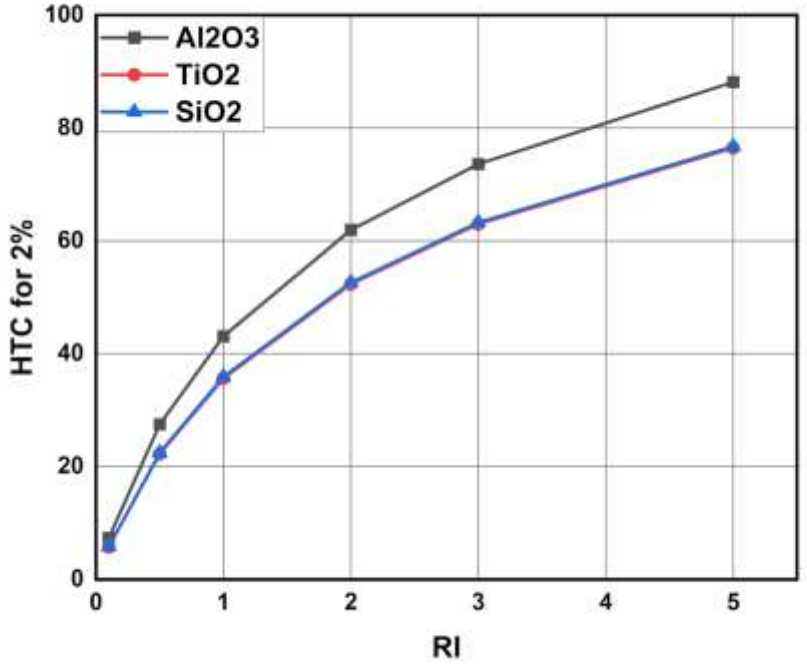

Graph-23: Heat transfer coefficient for various nanofluids at 2% volume concentration

Comparing results between Nanofluids:

- Here Aluminium oxide nanofluid has greater heat transfer coefficient than silicon oxide or titanium oxide of around 108.36 vs 79.270
- Water based Silicon oxide and Titanium oxide nanofluids has almost very same thermo-physical properties difference between those values is very less Nearly(HTC=79.270).
- As volume concentration increases gap between Aluminium-oxide nanofluids and silicon oxide nanofluid increasing, showing that as volume concentration is increasing, Aluminium oxide is showing greater sensitivity and providing higher heat transfer coefficient.

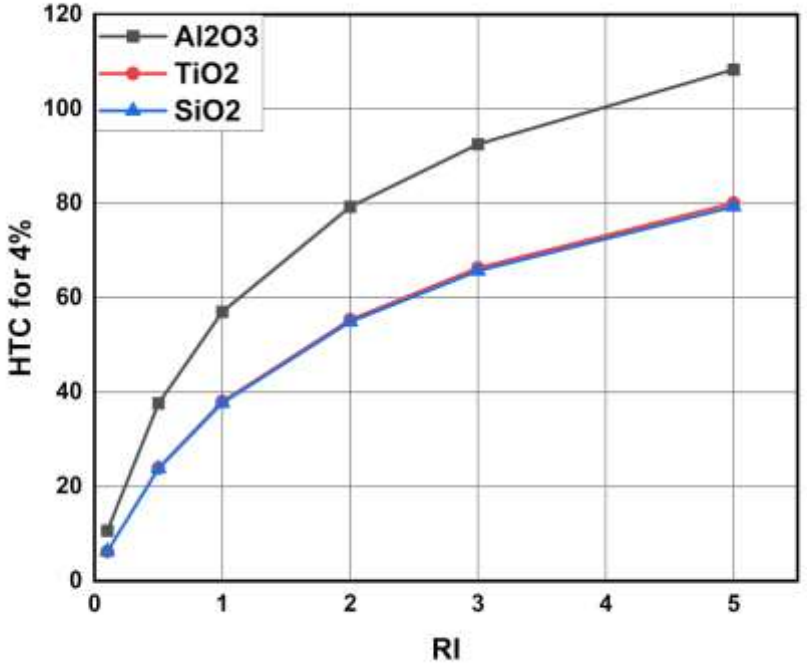

Graph-24: Heat transfer coefficient for various nanofluids at 4% volume concentration

Comparing results between Nanofluids:

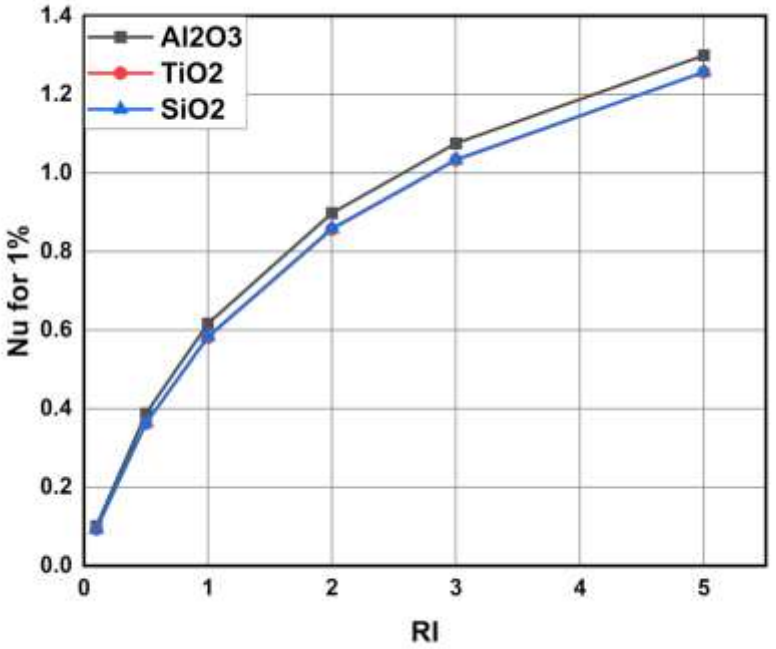

Graph-25: Nusselt Number for various nanofluids at 1% volume concentration

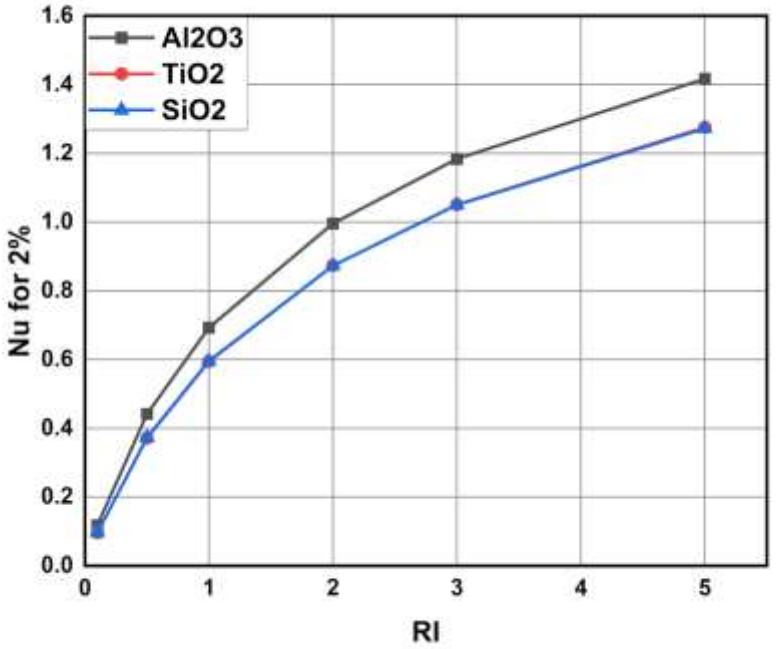

Graph-26: Nusselt Number for various nanofluids at 2% volume concentration

Comparing results between Nanofluids:

- Here water + aluminium oxide based has higher Nusselt number among the other two nanofluids.
- For Aluminium oxide nanofluid at 1% volume concentration , Nusselt number is varying from 0 to 1.4, at 2% volume concentration Nusselt number is varying from 0 to 1.6 and at 4% volume concentration Nusselt number is varying from 0 to 1.8.
- Where as for titanium and silicon oxide nanofluids has it is varying from 0 to 1.4 at all concentrations and values for both nanofluids are very close to each other.
- Comparatively Silicon oxide-water based nanofluid has lower Nusselt number.

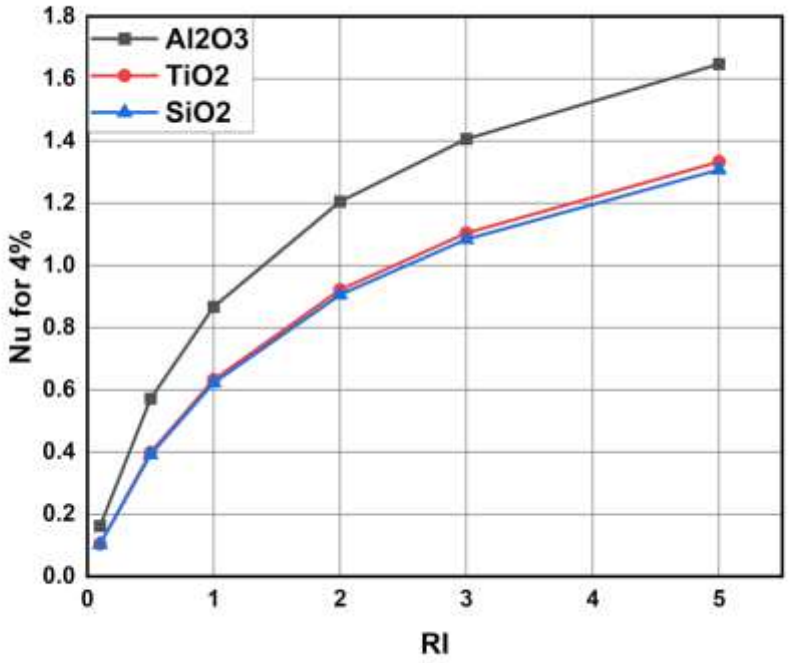

Graph-27: Nusselt Number for various nanofluids at 4% volume concentration

Comparing results between Nanofluids:

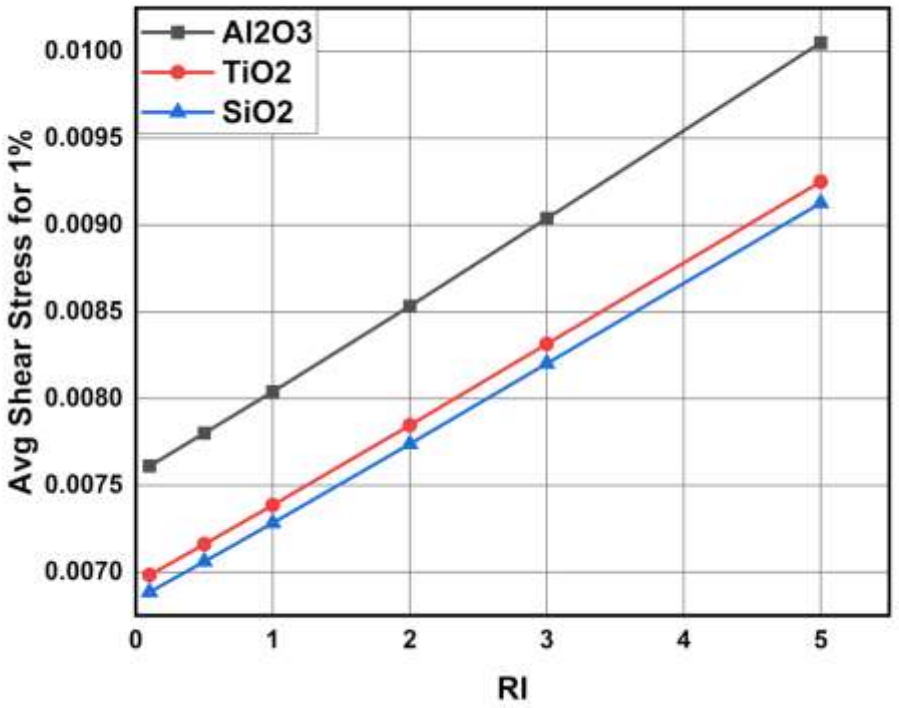

Graph-28: Average shear stress for various nanofluids at 1% volume concentration

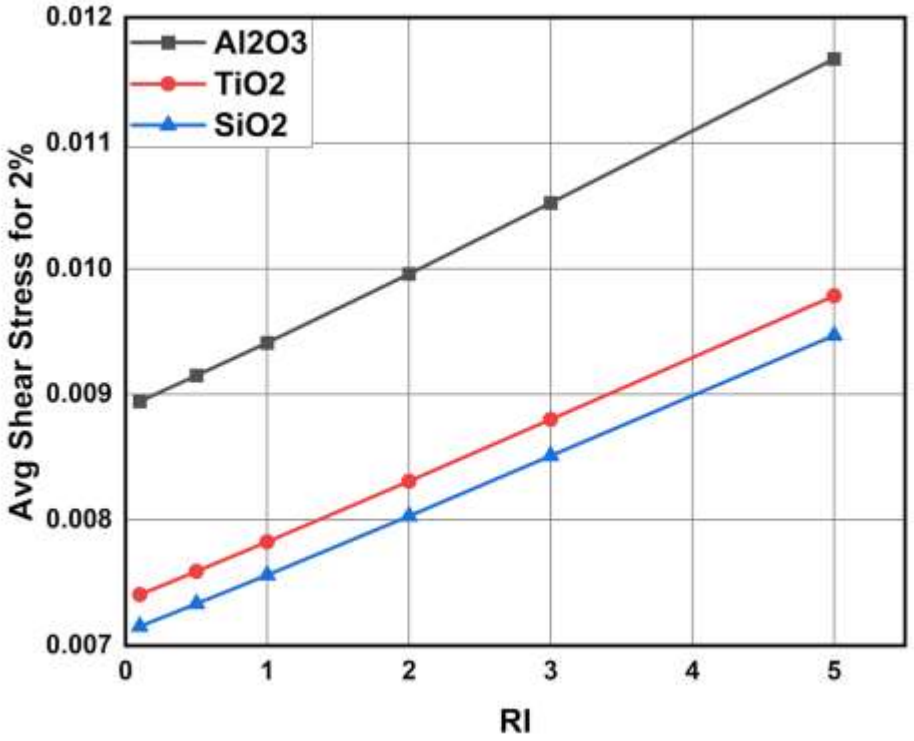

Graph-29: Average shear stress for various nanofluids at 2% volume concentration

Comparing results between Nanofluids:

- Along with heat transfer coefficient Aluminum oxide nanofluid also has higher shear stress around the walls of the duct (0.0169)
- As concentration increases gap between silicon oxide and titanium oxide increases and at 4% volume concentration titanium oxide has higher shear stress which is undesirable.(0.0113 vs 0.0102)
- Silicon oxide nanofluid is giving us the very less shear stress. 0.0102

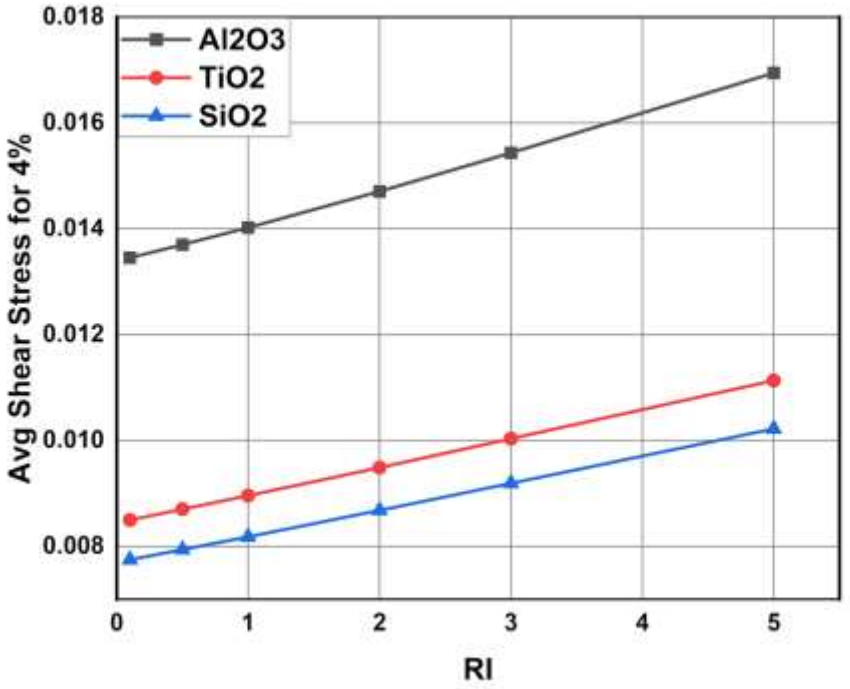

Graph-30: Average shear stress for various nanofluids at 4% volume concentration

Comparing results between Nanofluids:

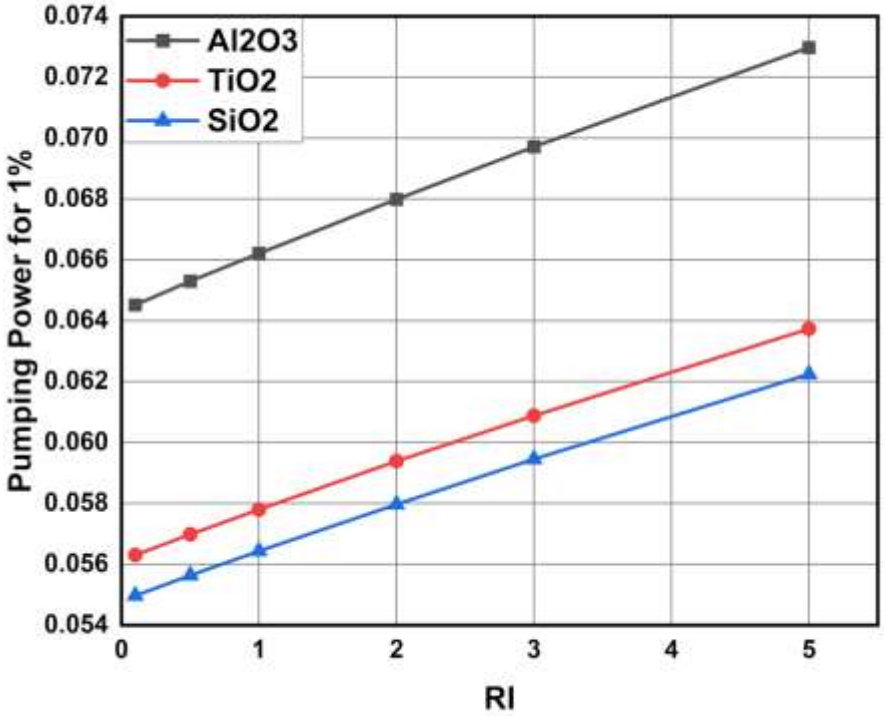

Graph-31: Pumping power for various nanofluids at 1% volume concentration

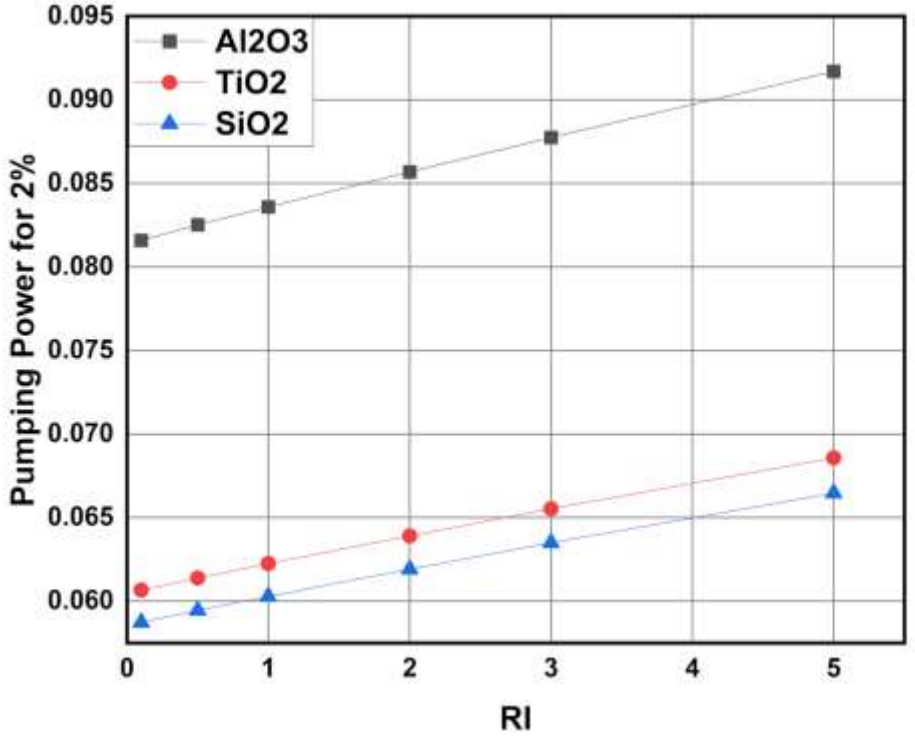

Graph-32: Pumping power for various nanofluids at 2% volume concentration

Comparing results between Nanofluids:

- Pumping power required for Water based Aluminium oxide nanofluid is (0.1685 at 4 % concentration) more compared to silicon oxide and titanium oxide nanofluids.
- Pumping power required for Titanium oxide nanofluid is more than that required for silicon oxide nanofluid at lower volume concentrations. (0.07543 vs 0.07274)
- As concentration increases Silicon oxide having pumping power of than that of Titanium oxide nanofluid (0.0818 vs 0.0852)

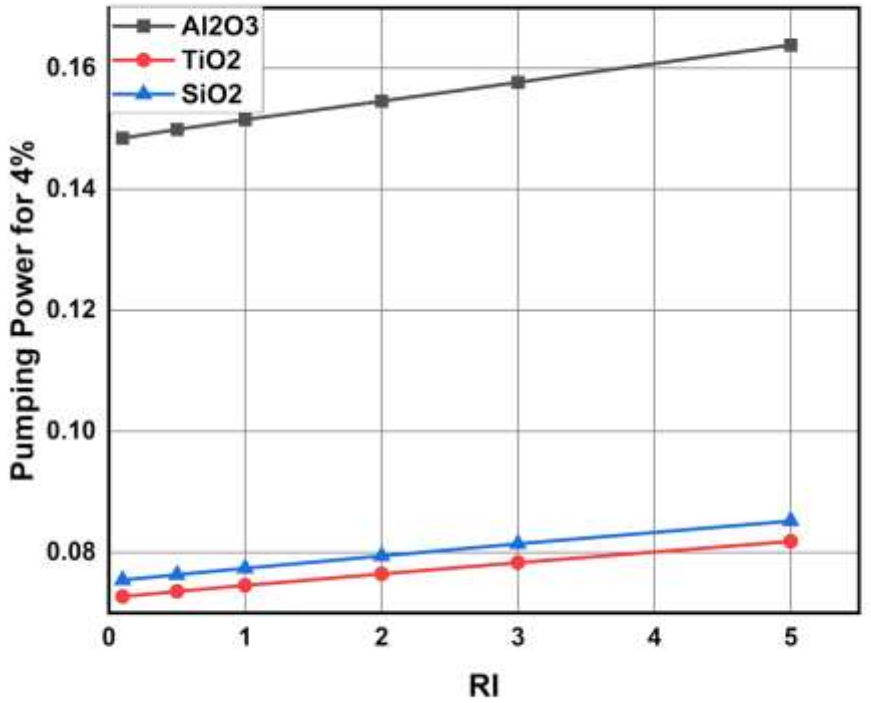

Graph-33: Pumping power for various nanofluids at 4% volume concentration

Contours of Aluminium oxide nanofluid:

- Here in the contours we can see the vortex formations in fluids
- Vortex are formed due to the pressure or velocity differences
- Due to Vortex formation fluid gets sucked in vortex centre and mixing of fluid happens
- Due to mixing and holding of fluids heat transfer increases.

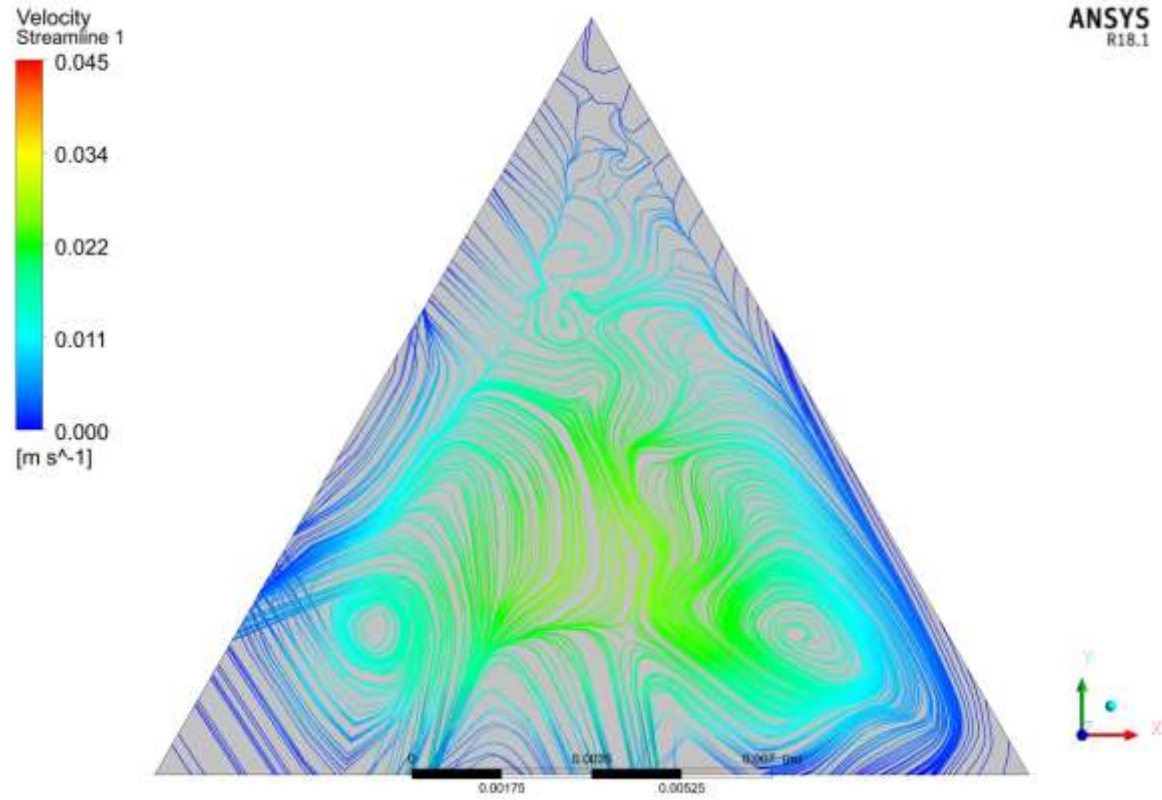

Figure-3: Velocity Streamline at midpoint(1000mm) at 4% volume concentration and Richardson number=5

Contours of Titanium oxide nanofluid:

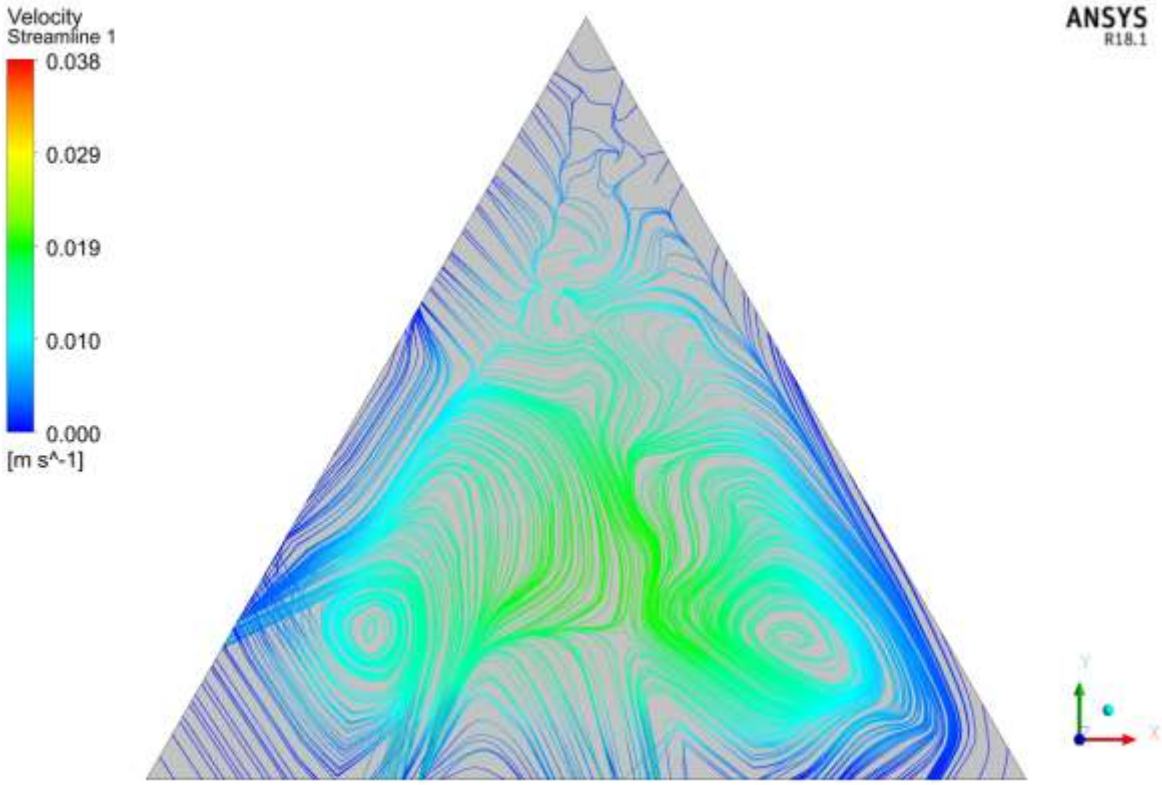

Figure-4: Velocity Streamline at midpoint(1000mm) at 0% volume concentration and Richardson number=5

- When the richardson number and volume concentrations are increasing the vortex are moving towards the wall surfaces.
- When the vortex are formed near the wall more heat near the wall, more fluid gets into the vortex and better mixing and holding takes place.

Contours of Silicon oxide nanofluid:

- Here aluminum oxide nanofluid is having higher stream line velocities.
- Whereas for silicon oxide and titanium oxide contours are close to each other which gives very similar properties.

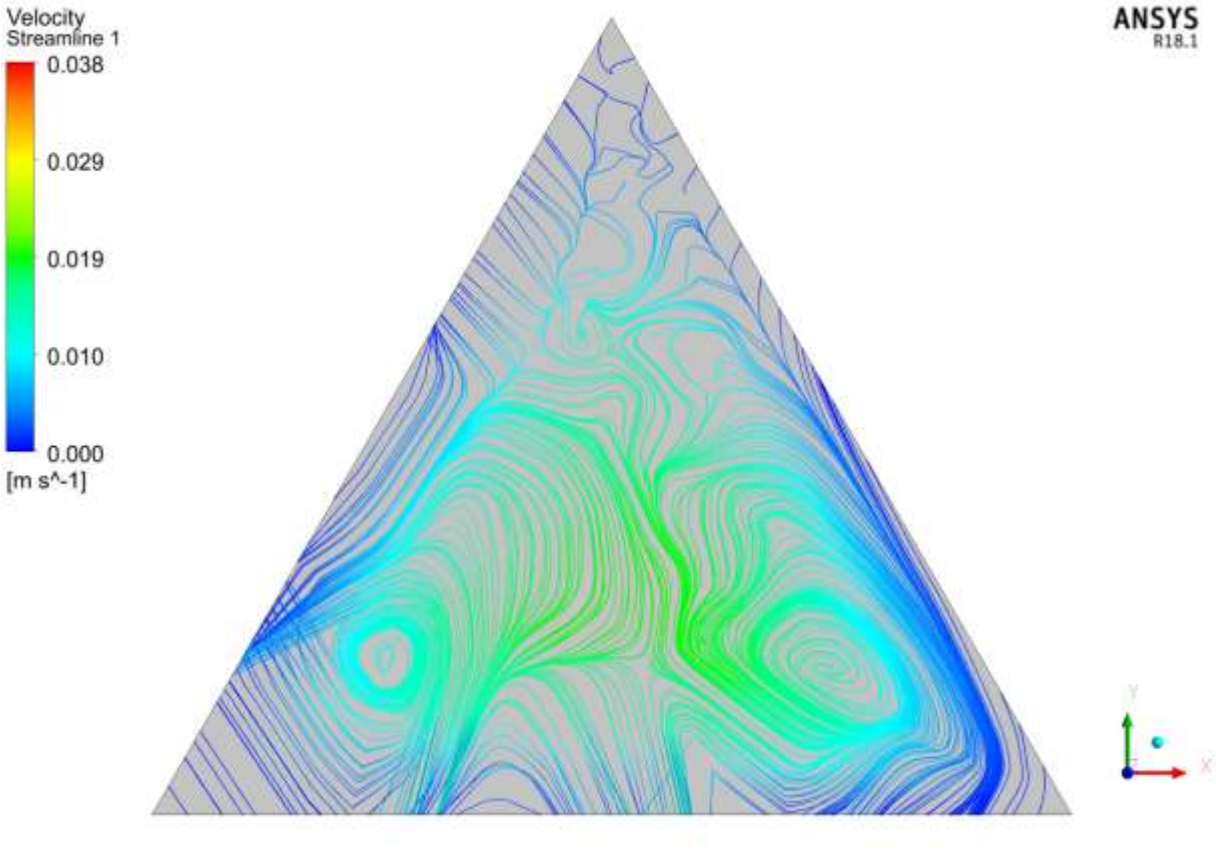

Figure-5: Velocity Streamline at midpoint(1000mm) at 0% volume concentration and Richardson number=5

ANALYSIS OF DIFFERENT DUCT GEOMETRIES

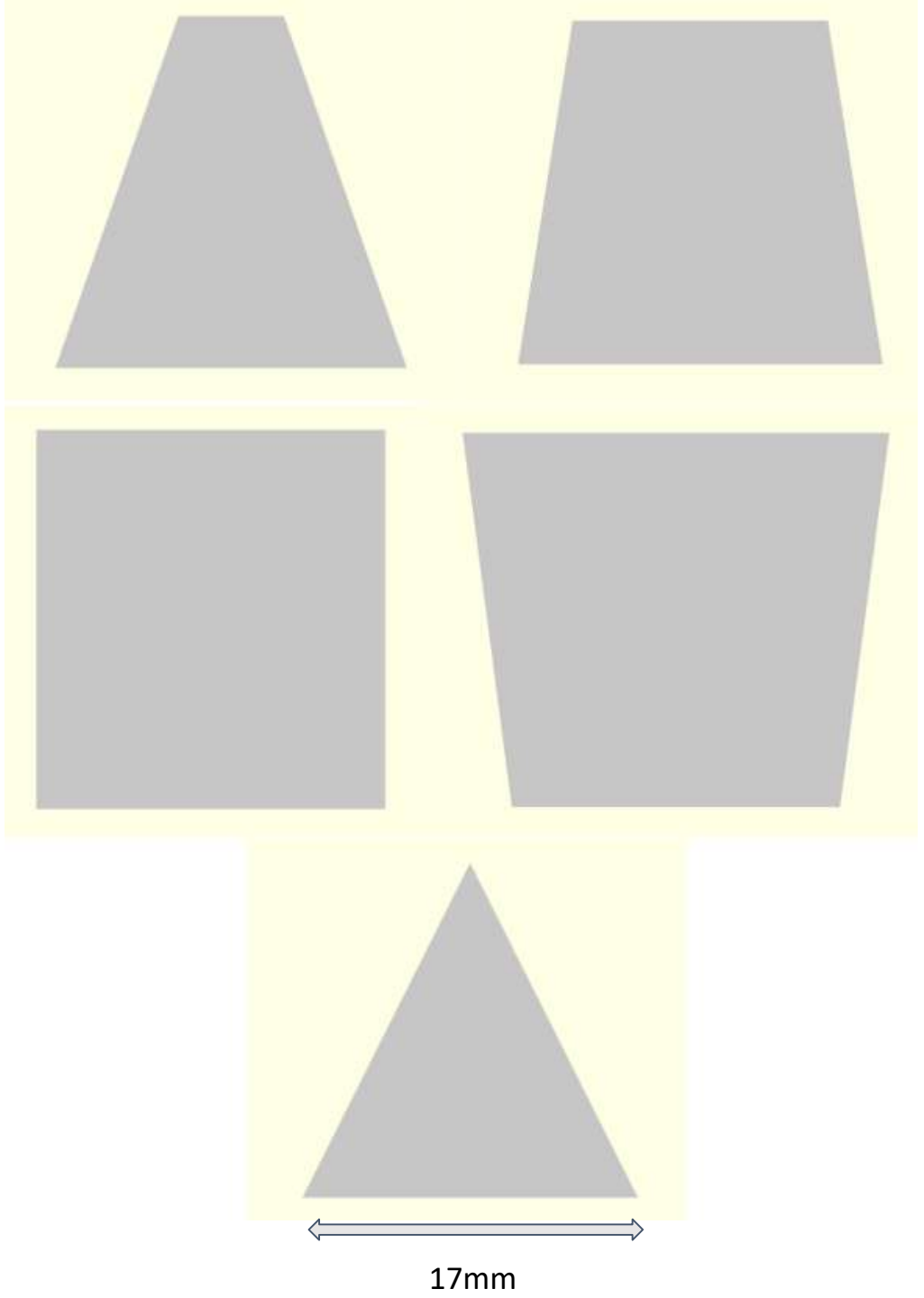
14.722 mm
17mm

Grid Independent Analysis of Trapezoidal Duct having 70 degrees angle

mesh size	no of elements	nusselt number
2	40000	0.633304523
1.5	79680	0.635467839
1	287856	0.630526466
0.75	722631	0.6247152429
0.6	1352416	0.6208621441
0.55	1675520	0.6197939698
0.5	2478760	0.618074539
0.4	4672512	0.617018928

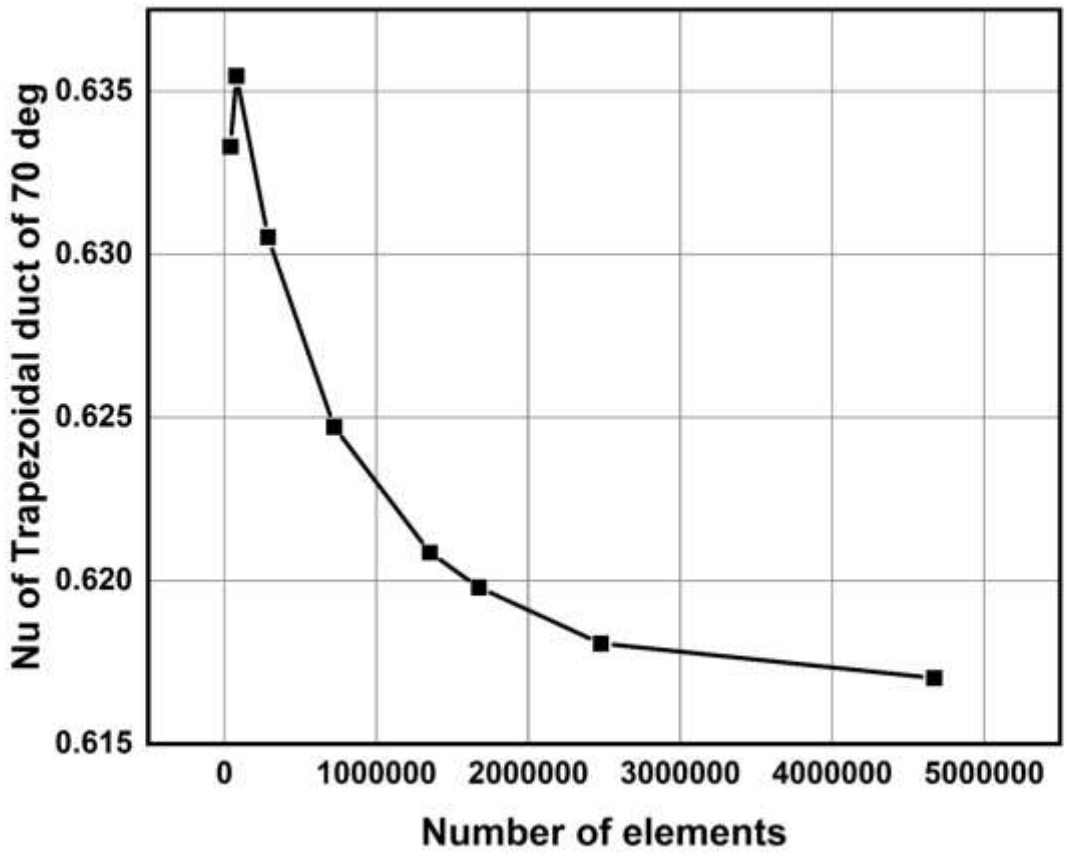

Graph-34: Validation of Trapezoidal Duct having 70 degrees angle

Grid Independent Analysis of Trapezoidal Duct having 80 degrees angle

mesh size	no of elements	nusselt number
2.5	56000	0.6504
1.5	119520	0.6515
1.25	209748	0.6487
1	419790	0.64395
0.75	1006620	0.63829
0.6	1798968	0.63571
0.5	3480000	0.63358
0.4	6656004	0.63237

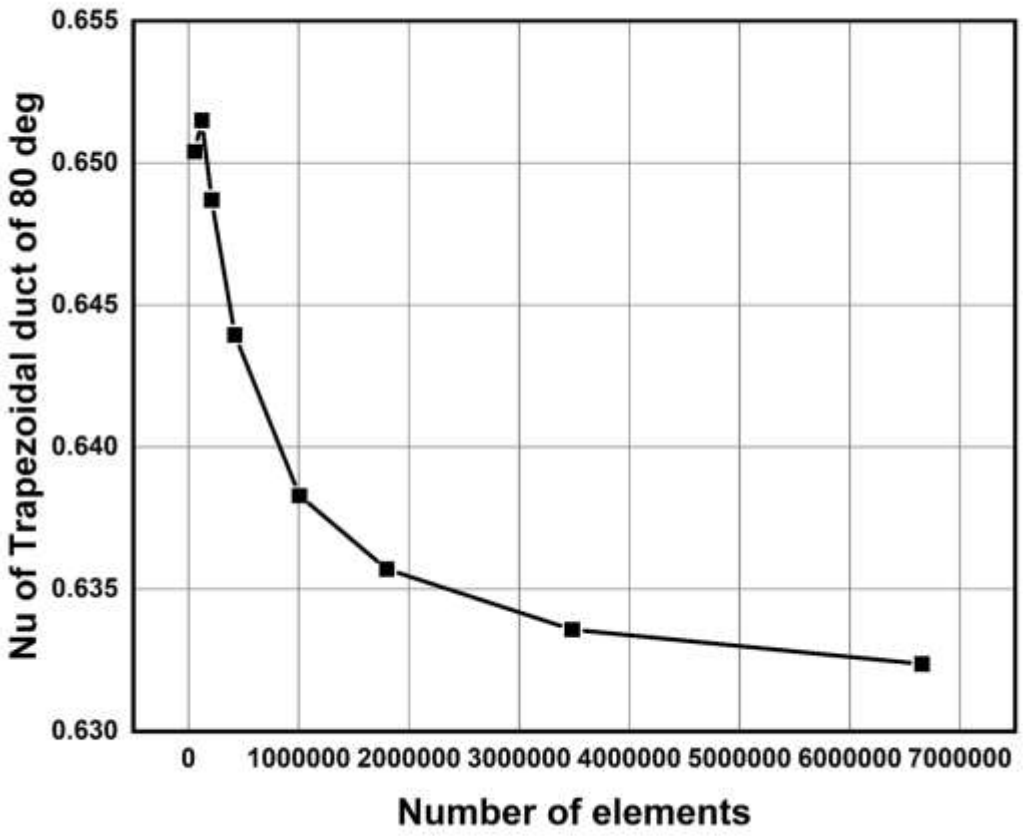

Graph-35: Validation of Trapezoidal Duct having 80 degrees angle

Grid Independent Analysis of Trapezoidal Duct having 90 degrees angle

mesh size	no of elements	nusselt number
3.5	11420	0.0938435343
2.5	33348	0.093741005
2	63000	0.09358306533
1.5	145640	0.0933168844
1	509490	0.0930056114
0.9	673968	0.0929714405
0.8	940086	0.0929351256
0.75	1216700	0.0929104523
0.7	1421280	0.092901005
0.6	2176608	0.0928785092
0.55	2728440	0.0928785092
0.5	3944000	0.092858727

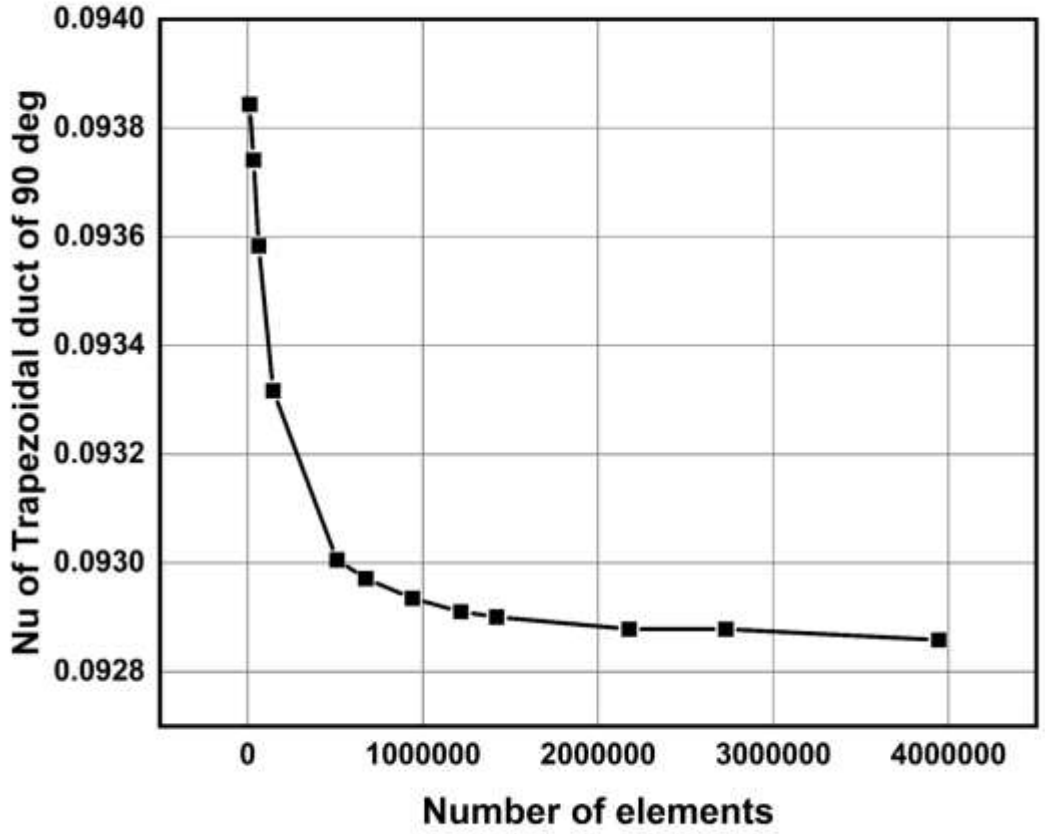

Graph-36: Validation of Trapezoidal Duct having 90 degrees angle

Grid Independent Analysis of Trapezoidal Duct having 100 degrees angle

mesh size	no of elements	nusselt number
2.5	38256	0.0938435343
2	80000	0.093741005
1.5	172900	0.09358306533
1	569715	0.0933168844
0.75	1377480	0.0930056114
0.6	2509056	0.0929714405
0.5	4680000	0.0929351256

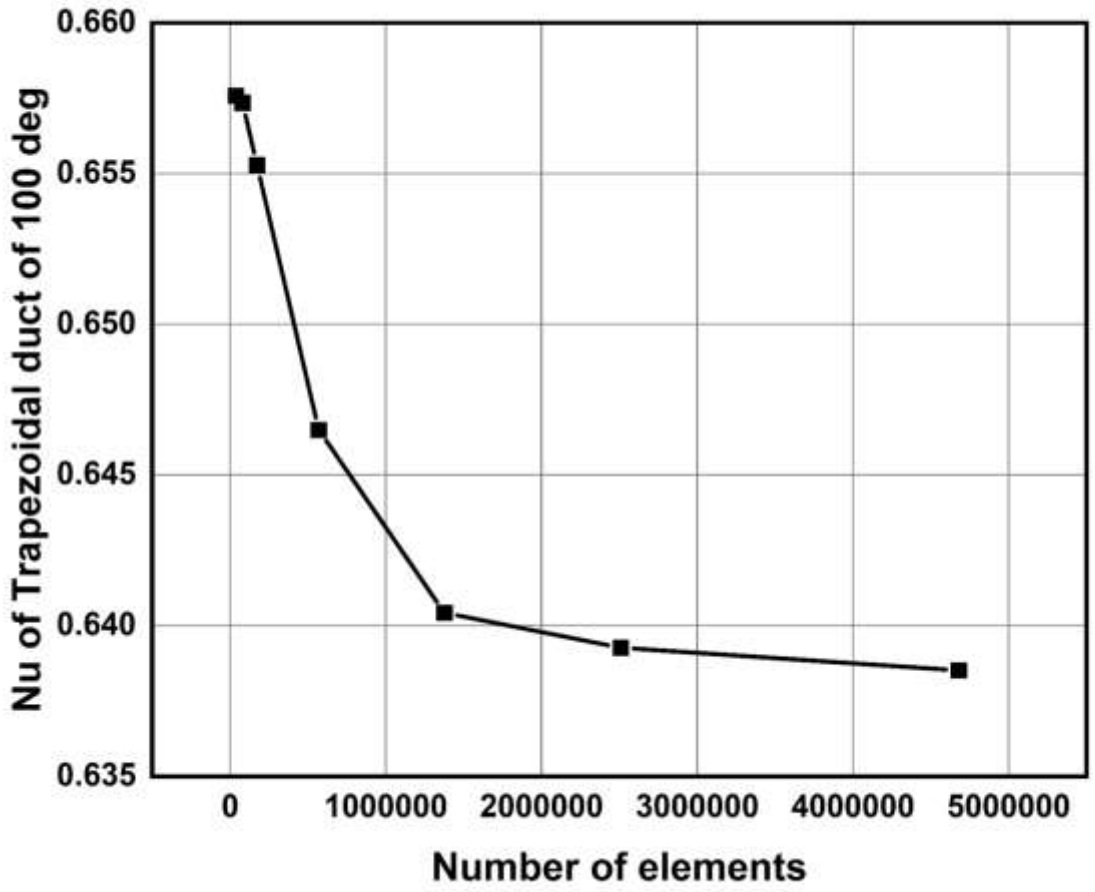

Graph-37: Validation of Trapezoidal Duct having 100 degrees angle

Heat Transfer Coefficient for different Richardson numbers and different volume concentration values in Duct with 70 Degrees angle:

- HTC increases with increase in volume concentration of nanoparticles.
- HTC for different Richardson's number ranges from 36.77633 to 127.4623
- The percentage increase of HTC at 1%,2%,4% with respective to the HTC at 0% is calculated by:
  % Change = (HTC **at x% -** HTC **at 0%) /** HTC **at 0%**
- For Richard number 1:
  % change for 1% = 12.51 % for 2% =26.975% for 4%=69.42%
- For Richard number 3:
  % change for 1%= 10.062 % for 2% = 21.46% for 4%:53.41%
- For Richard number 5:
  % change for 1% = 9.17% for 2% = 19.513% for 4%: 48.24%
- As Richardson number is increasing HTC increases and after a certain Richardson number it is becoming constant.

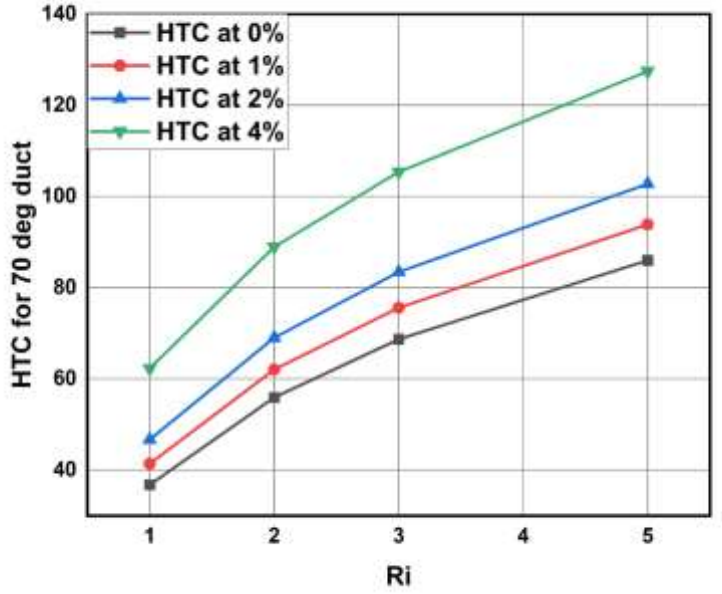

Graph-38: Richardson number vs average heat transfer coefficient values for different volume concentrations.

Heat Transfer Coefficient for different Richardson numbers and different volume concentration values in Duct with 80 Degrees angle:

- HTC increases with increase in volume concentration of nanoparticles.
- HTC for different Richardson's number ranges from 37.89921 to 135.5654
- The percentage increase of HTC at 1%,2%,4% with respective to the HTC at 0% is calculated by:
  % Change = (HTC **at x% -** HTC **at 0%) /** HTC **at 0%**
- For Richard number 1:
  % change for 1% = 12.68 % for 2% =27.32% for 4% =70.25%
  For Richard number 3:
  % change for 1%= 10.183% for 2% = 21.58% for 4%: 55.34%
- For Richard number 5:
  % change for 1% = 9.249 for 2% = 19.675% for 4%: 48.60%
- As Richardson number is increasing HTC increases and after a certain Richardson number it is becoming constant.

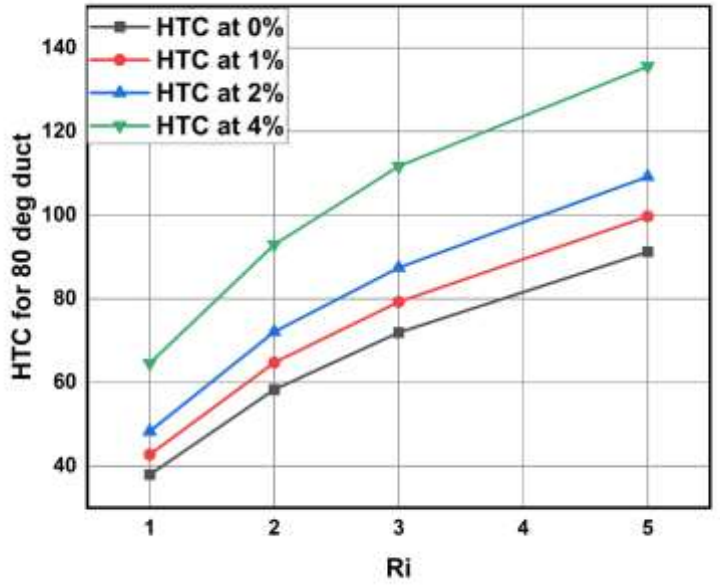

Graph-39: Richardson number vs average heat transfer coefficient values for different volume concentrations.

Heat Transfer Coefficient for different Richardson numbers and different volume concentration values in Rectangular duct:

- HTC increases with increase in volume concentration of nanoparticles.
- HTC for different Richardson's number ranges from 38.21672 to 138.0554
- The percentage increase of HTC at 1%,2%,4% with respective to the HTC at 0% is calculated by:
  % Change = (HTC **at x% -** HTC **at 0%) /** HTC **at 0%**
- For Richard number 1:
  % change for 1% = 12.74 % for 2% =27.42% for 4% =70.34%
- For Richard number 3:
  % change for 1%= 2.1295% for 2% = 4.217% for 4%: 8.66%
- For Richard number 5:
  % change for 1% = 10.34 for 2% = 22.049% for 4%:54.86%

As Richardson number is increasing HTC increases and after a certain Richardson number it is becoming constant.

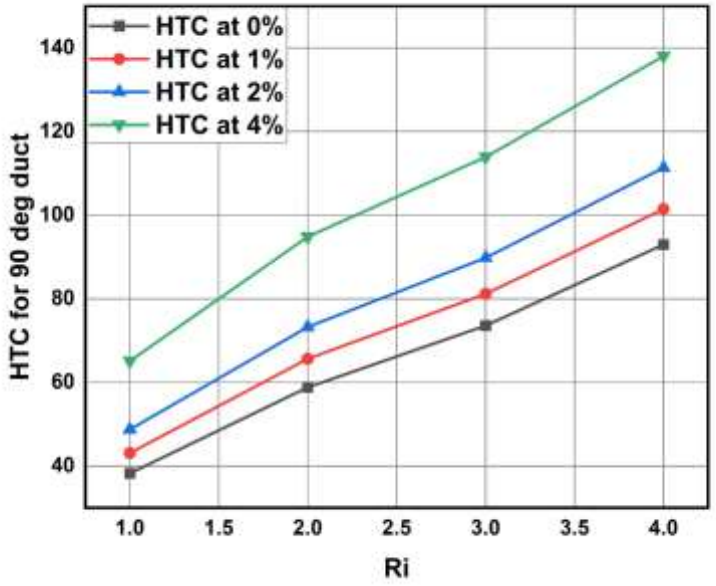

Graph-40: Richardson number vs average heat transfer coefficient values for different volume concentrations.

Heat Transfer Coefficient for different Richardson numbers and different volume concentration values in Duct with 100 Degrees angle:

- HTC increases with increase in volume concentration of nanoparticles.
- HTC for different Richardson's number ranges from 38.16433 to 138.594
- The percentage increase of HTC at 1%,2%,4% with respective to the HTC at 0% is calculated by:
  % Change = (HTC **at x% -** HTC **at 0%) /** HTC **at 0%**
- For Richard number 1:
  % change for 1% = 12.73 % for 2% =27.33% for 4% =70.31%
- For Richard number 3:
  % change for 1%= 10.350% for 2% = 22% for 4%: 54.61%
  For Richard number 5:
  % change for 1% = 9.307 for 2% = 19.05% for 4%: 48.24%
- As Richardson number is increasing HTC increases and after a certain Richardson number it is becoming constant.

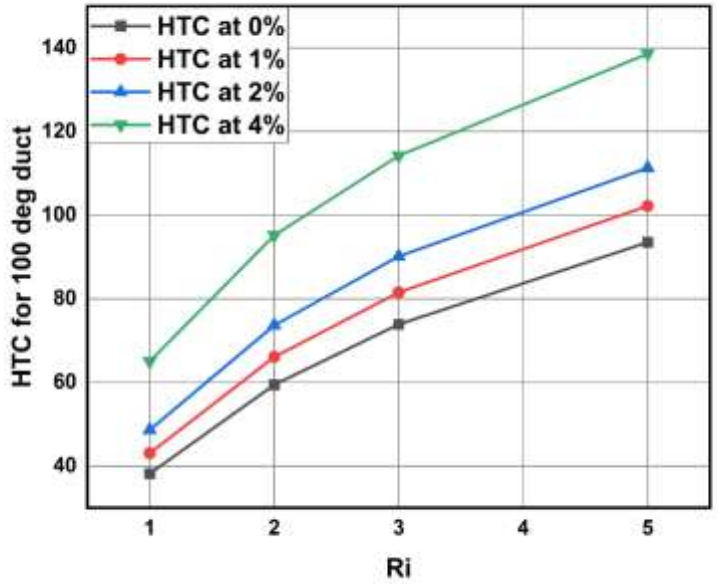

Graph-41: Richardson number vs average heat transfer coefficient values for different volume concentrations.

Comparing Heat Transfer Coefficients in different ducts:

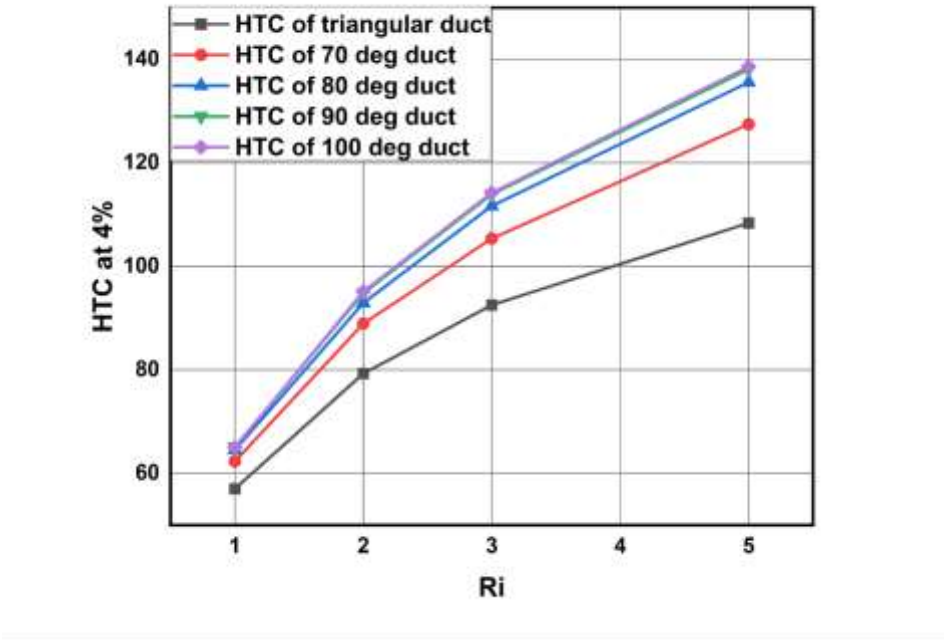

Graph-42:Heat Transfer Coefficient in different ducts

- Here Ducts with larger Angles is having greater Heat transfer coefficient values.
- Triangular duct is having least heat transfer coefficient values where as duct with 100 degrees is having highest heat transfer coefficient values.
- Duct with 100 degrees is having higher heat transfer coefficient of 138.594.

Nusselt Numbers for different Richardson numbers and different volume concentration values for Duct with 70 Degrees:

- Nusselt number increases with increase in concentration.
- Nu value for different Richardson's number ranges from 0.616018928 to 1.937117021
- The percentage increase of Nusselt number at 1%,2%,4% with respective to the Nusselt number at 0% is calculated by

  % Change = (Nu at x% - Nu at 0%) / Nu at 0%
- For Richardson number = 1:

  % Change at 1% = 7.987% % , 2% = 19.189% , 4% = 53.714%

  For Richardson number = 3:

  % Change at 1% = 5.638% , 2% =14.01% , 4% = 39.196%

  For Richardson number = 5:

  % Change at 1% =4.782% , 2% =12.184% , 4% = 34.49%

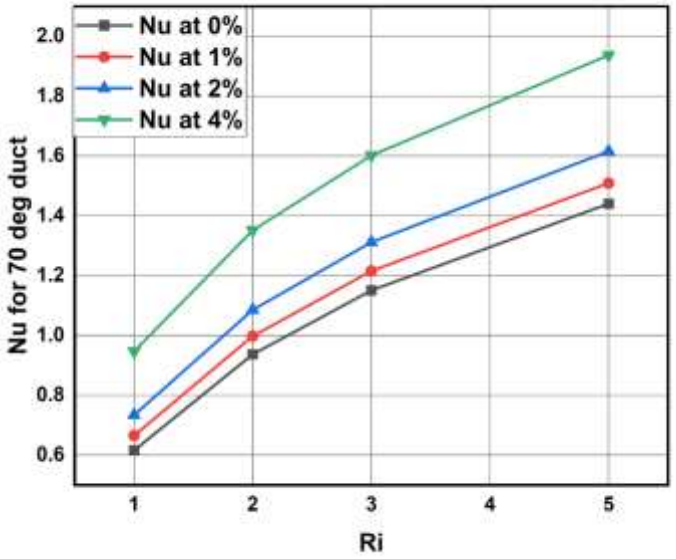

Graph-43: Richardson Number vs Nusselt Number values for different volume concentrations.

Nusselt Numbers for different Richardson numbers and different volume concentration values for Duct with 80 Degrees :

- Nusselt number increases with increase in concentration.
- Nu value for different Richardson's number ranges from 0.6348276382 to 2.060264438
- The percentage increase of Nusselt number at 1%,2%,4% with respective to the Nusselt number at 0% is calculated by

  % Change = (Nu at x% - Nu at 0%) / Nu at 0%
- For Richardson number = 1:

  % Change at 1% = 8.154% % , 2% = 19.51% , 4% = 54.47%

  For Richardson number = 3:

  % Change at 1% = 5.7543% , 2% =14.128% , 4% = 40.94%
- For Richardson number = 5:

  % Change at 1% = 4.8579% , 2% =12.33% , 4% = 34.82%

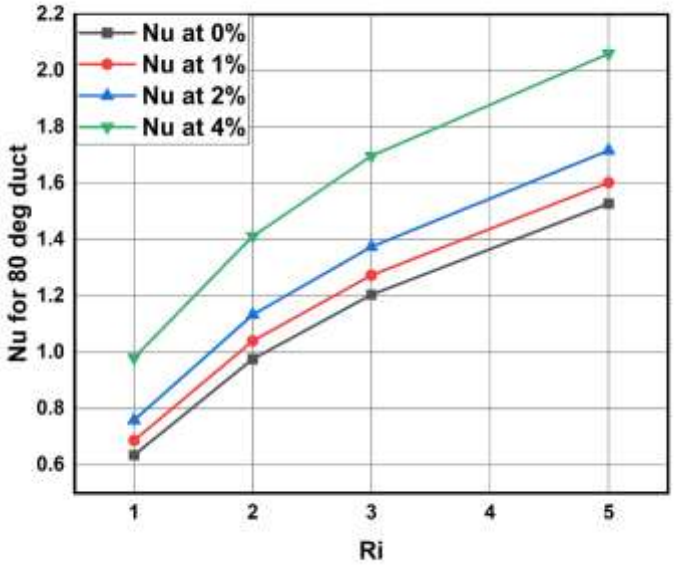

Graph-44: Richardson Number vs Nusselt Number values for different volume concentrations.

Nusselt Numbers for different Richardson numbers and different volume concentration values for Duct with 90 Degrees :

- Nusselt number increases with increase in concentration.
- Nu value for different Richardson's number ranges from 0.6401460637 to 2.09810638
- The percentage increase of Nusselt number at 1%,2%,4% with respective to the Nusselt number at 0% is calculated by

  % Change = (Nu at x% - Nu at 0%) / Nu at 0%
- For Richardson number = 1:

  % Change at 1% = 8.212% , 2% =19.602% , 4% = 54.556%
- For Richardson number = 3:

  % Change at 1% = 5.908% , 2% =14.565% , 4% = 40.508%
- For Richardson number = 5:

  % Change at 1% =4.753% , 2% =12.41% , 4% = 34.763%

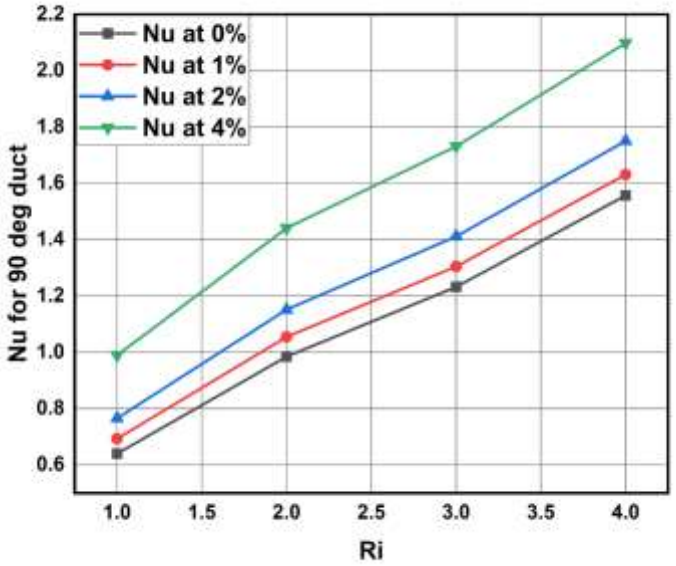

Graph-45: Richardson Number vs Nusselt Number values for different volume concentrations.

Nusselt Numbers for different Richardson numbers and different volume concentration values for Duct with 100 Degrees :

- Nusselt number increases with increase in concentration.
- Nu value for different Richardson's number ranges from 0.6392685092 to 2.106291793
- The percentage increase of Nusselt number at 1%,2%,4% with respective to the Nusselt number at 0% is calculated by

  % Change = (Nu at x% - Nu at 0%) / Nu at 0%
- For Richardson number = 1:

  % Change at 1% = 8.19% % , 2% = 19.527% , 4% = 54.526%

  For Richardson number = 3:

  % Change at 1% = 5.91% , 2% =14.518% , 4% = 40.28%
- For Richardson number = 5:

  % Change at 1% =4.914% , 2% =11.750% , 4% =34.499%

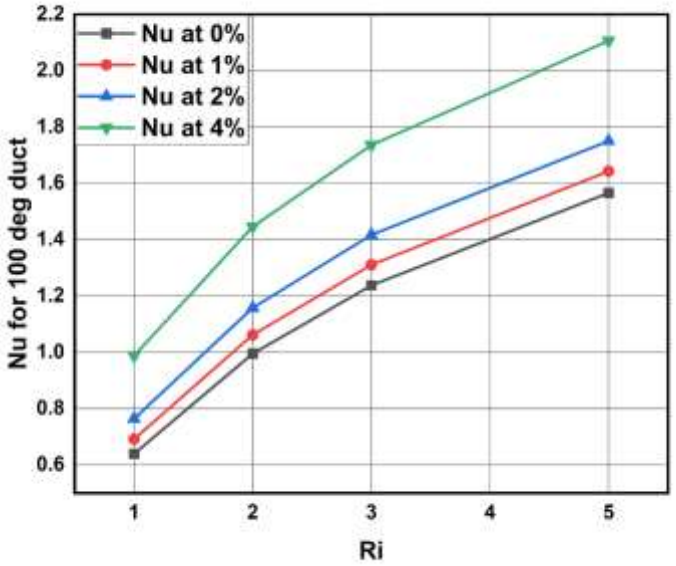

Graph-46: Richardson Number vs Nusselt Number values for different volume concentrations.

Comparing Nusselt Number in different ducts:

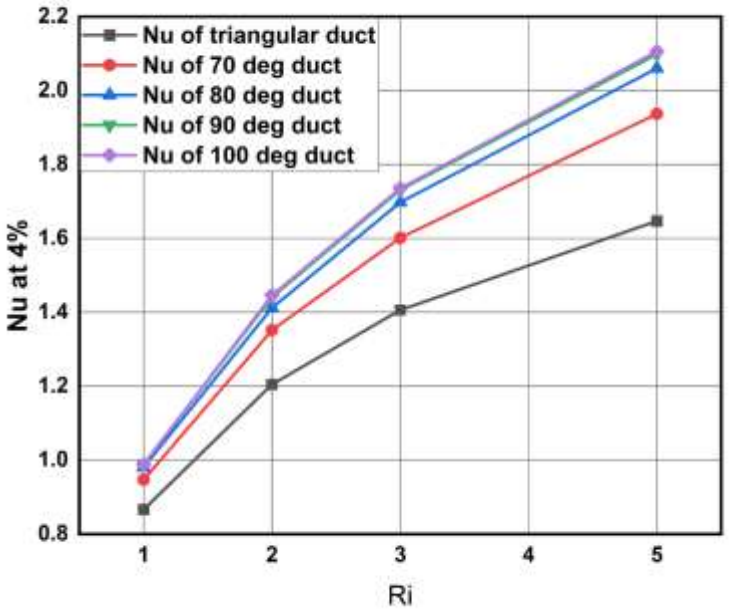

Figure-47: Nu for various ducts

- Similar to heat transfer coefficient, Nusselt Number also increases as the angle of duct is increasing.
- Nu of 100 degrees angle duct is high(2.106)
- Nusselt Number for Duct with 100 degrees is varying from 0.987 to 2.106.
- Triangular duct is having least Nusselt number among all the ducts
- Nusselt Number of Triangular duct is varying from 0.866 to 1.646.

Average Shear stresses for different Richardson numbers and different volume concentration values for Duct with 70 Degrees:

- As richardson's number is increasing average shear stress on walls also increasing.
- Average shear stress for different richardson's number ranges from 0.006001106 to 0.01415043
- The percentage change in avg shear stress compared with 0% concentration as reference are as follows
  % Change = (value at x% - value at 0%) / value at 0%
- For Richard number 1:
  % change for 1% =14.86% for 2% =35.006% for 4% = 102.98%
  For Richard number 3:
  % change for 1%= 14.609% for 2% = 34.064% for 4%: 98.89%
  For Richard number 5:
  % change for 1% = 14.398 for 2% = 33.356% for 4%: 95.793%

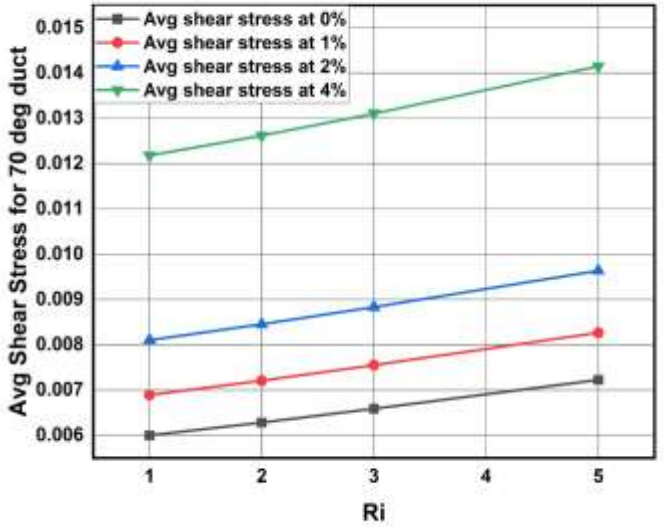

Graph-48: Richardson Number vs average Shear Stress values for different volume concentrations.

Average Shear stresses for different Richardson numbers and different volume concentration values for Duct with 80 Degrees :

- As richardson's number is increasing average shear stress on walls also increasing.
- Average shear stress for different richardson's number ranges from 0.005554949 to 0.01445394
- The percentage change in avg shear stress compared with 0% concentration as reference are as follows

  % Change = (value at x% - value **at 0%) /** value **at 0%**
- For Richard number 0.1:

  % change for 1% = 14.073% for 2% = 33.02 % for 4% = 96.8%
- For Richard number 2:

  % change for 1%= 13.783% for 2% = 31.8% for 4%: 90.48%
- For Richard number 5:

  % change for 1% = 13.728 for 2% = 31.262% for 4%: 87.889%

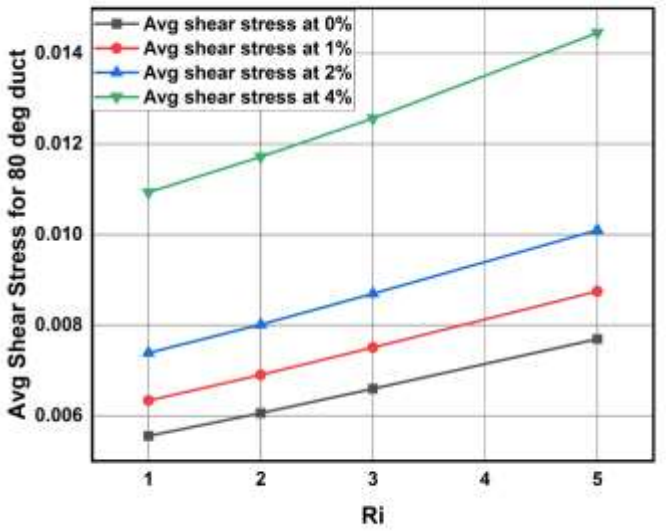

Graph-49: Richardson Number vs average Shear Stress values for different volume concentrations.

Average Shear stresses for different Richardson numbers and different volume concentration values for Duct with 90 Degrees :

- As richardson's number is increasing average shear stress on walls also increasing.
- Average shear stress for different richardson's number ranges from 0.005350876 to 0.01462316
- The percentage change in avg shear stress compared with 0% concentration as reference are as follows

  % Change = (value at x% - value **at 0%) /** value **at 0%**
- For Richard number 1:

  % change for 1% = 13.607% for 2% = 31.85% for 4% = 93.23

- For Richard number 3:

  % change for 1%= 13.38% for 2% = 30.716% for 4%:87.467%

  For Richard number 5:

  % change for 1% = 13.32 for 2% = 30.3% for 4%: 84.537%

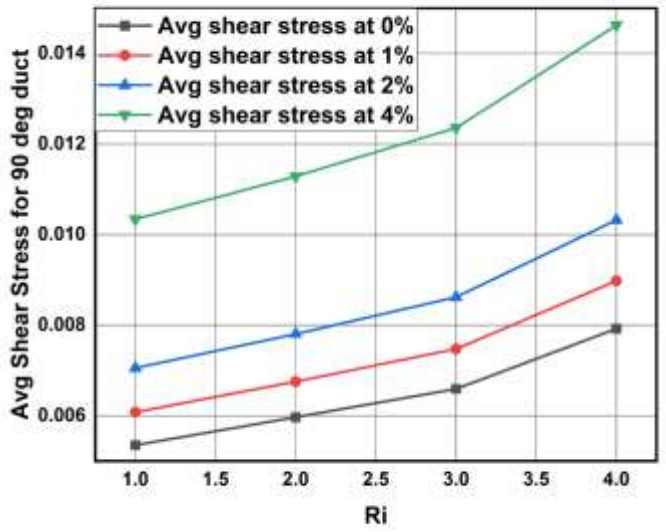

Graph-50: Richardson Number vs average Shear Stress values for different volume concentrations.

Average Shear stresses for different Richardson numbers and different volume concentration values for Duct with 100 Degrees :

- As richardson's number is increasing average shear stress on walls also increasing.
- Average shear stress for different richardson's number ranges from 0.005206848 to 0.01461829
- The percentage change in avg shear stress compared with 0% concentration as reference are as follows

  % Change = (value at x% - value **at 0%) /** value **at 0%**
- For Richard number 1:

  % change for 1% = 13.44% for 2% = 31.44% for 4% = 91.705%
- For Richard number 3:

  % change for 1%= 13.256% for 2% =30.39% for 4%: 86.301%
- For Richard number 5:

  % change for 1% = 13.32 for 2% = 29.367% for 4%: 84.062%

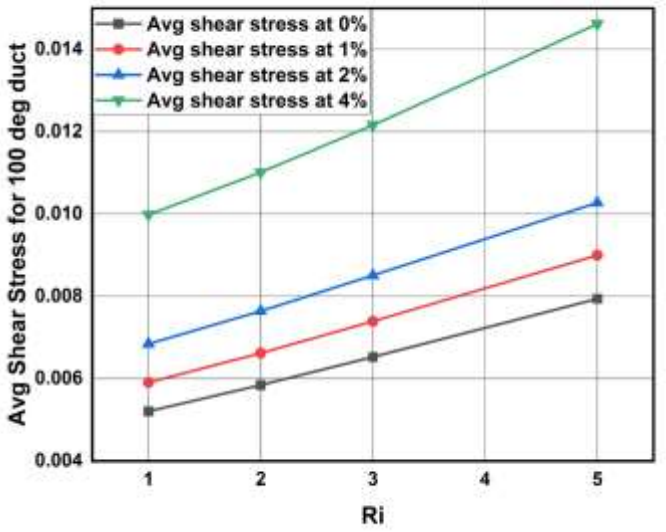

Graph-51: Richardson Number vs average Shear Stress values for different volume concentrations.

Comparing Average Shear Stress in different ducts:

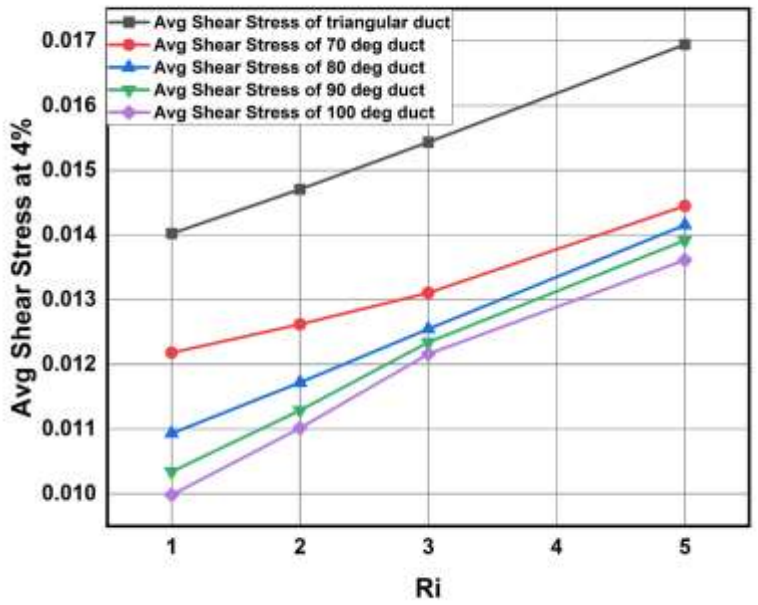

Graph-52: Average Shear Stress for various ducts

- On contrast to Nusselt number, Average shear stress values are increasing with the decrease in the angle of the duct.
- Triangular duct is having the higher shear stress compared to all geometries. It's value is ranging from 0.169 to 0.136.
- Trapezoidal duct with 100 degrees is having least shear stress among all geometries and at every richardson number.

Pumping Power for different Richardson numbers and different volume concentration values for Duct with 70 degrees:

- Here as Heat transfer is increasing power required to pump the fluid into duct also increasing.
- Pumping power is increasing linearly with respective to Richardson's number.
- The range of pumping power is 0.0373876682 and 0.11035
- The percentage change with 0% concentration as reference are as follow

  % Change = (value at x% - value **at 0%) /** value **at 0%**
- For Richardson Number = 1:

  % change at 1% = 3.87% at 2% = 11% 4% = 42%
- For Richardson Number = 3:

  % change at 1% = 9.025% at 2% = 16.44% at 4% = 49.392%
- For Richardson Number = 5:

  % change at 1% = 3.728% at 2% = 10.76% at 4% = 41.984%
- At higher concentrations and at higher Richardson's number pumping power required is becoming more.

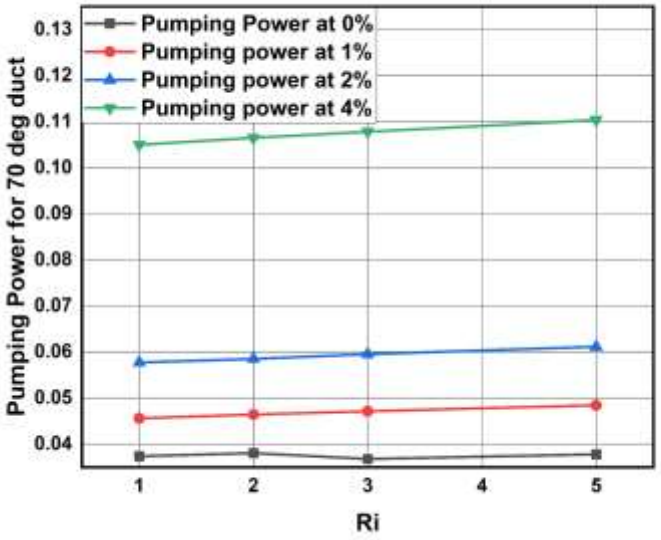

Graph-53: Richardson Number vs Pumping Power for different volume concentrations.

Pumping Power for different Richardson numbers and different volume concentration values for Duct with 80 degrees :

- Here as Heat transfer is increasing power required to pump the fluid into duct also increasing.
- Pumping power is increasing linearly with respective to Richardson's number.
- The range of pumping power is 0.0272 and 0.08541
- The percentage change with 0% concentration as reference are as follow

  % Change = (value at x% - value **at 0%) /** value **at 0%**
- For Richardson Number = 1:

  % change at 1% = 3.87% at 2% = 11% 4% = 42%
- For Richardson Number = 3:

  % change at 1% = 9.025% at 2% = 16.44% at 4% = 49.392%
- For Richardson Number = 5:

  % change at 1% = 3.728% at 2% = 10.76% at 4% = 41.984%
- At higher concentrations and at higher Richardson's number pumping power required is becoming more.

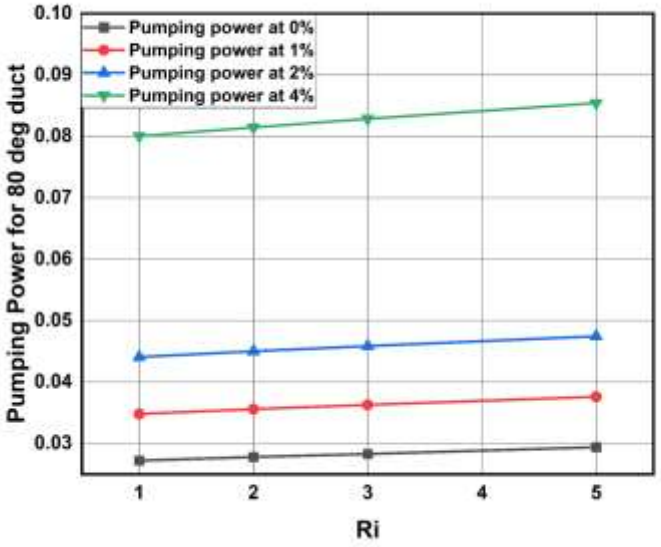

Graph-54: Richardson Number vs Pumping Power for different volume concentrations.

Pumping Power for different Richardson numbers and different volume concentration values for Duct with 90 degrees :

- Here as Heat transfer is increasing power required to pump the fluid into duct also increasing.
- Pumping power is increasing linearly with respective to Richardson's number.
- The range of pumping power is 0.0244088803 and 0.0732867526
- The percentage change with 0% concentration as reference are as follow
  % Change = (value at x% - value **at 0%) /** value **at 0%**
- For Richardson Number = 1:
  % change at 1% = 3.87% at 2% = 11% 4% = 42%
- For Richardson Number = 3:
  % change at 1% = 9.025% at 2% = 16.44% at 4% = 49.392%
- For Richardson Number = 5:
  % change at 1% = 3.728% at 2% = 10.76% at 4% = 41.984%
- At higher concentrations and at higher Richardson's number pumping power required is becoming more

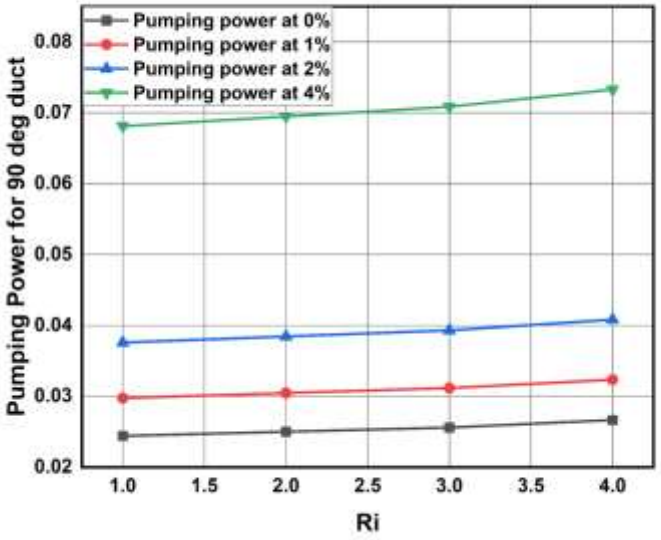

Graph-55: Richardson Number vs Pumping Power for different volume concentrations.

Pumping Power for different Richardson numbers and different volume concentration values for Duct with 100 degrees :

- Here as Heat transfer is increasing power required to pump the fluid into duct also increasing.
- Pumping power is increasing linearly with respective to Richardson's number.
- The range of pumping power is 0.021 and 0.0666
- The percentage change with 0% concentration as reference are as follow

  % Change = (value at x% - value **at 0%) /** value **at 0%**
- For Richardson Number = 1:

  % change at 1% = 3.87% at 2% = 11% 4% = 42%
- For Richardson Number = 3:

  % change at 1% = 9.025% at 2% = 16.44% at 4% = 49.392%
- For Richardson Number = 5:

  % change at 1% = 3.728% at 2% = 10.76% at 4% = 41.984%
- At higher concentrations and at higher Richardson's number pumping power required is becoming more.

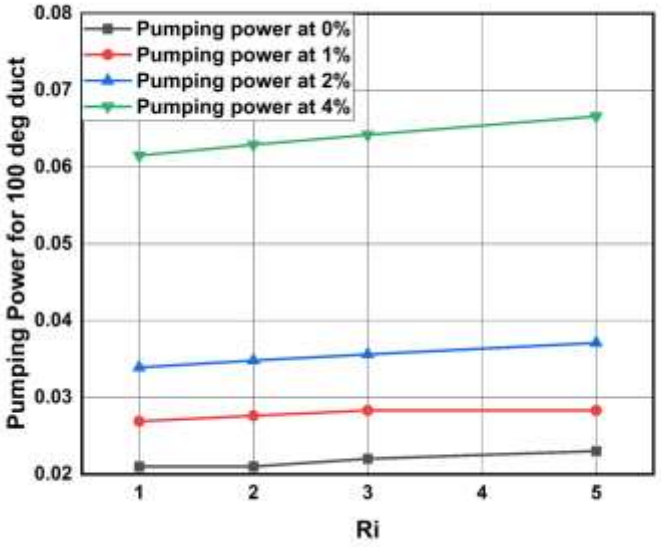

Graph-56: Richardson Number vs Pumping Power for different volume concentrations.

Comparing Pumping Power in different ducts:

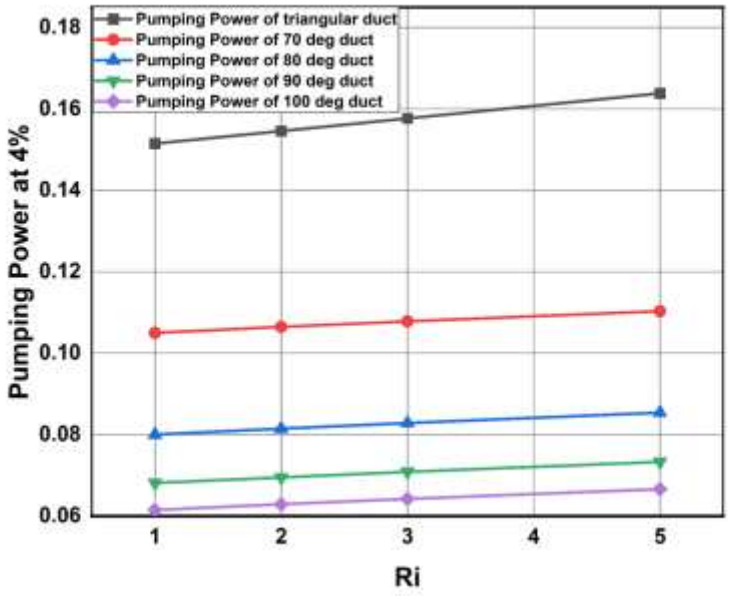

Figure-57: Pumping power for various ducts

- Pumping power required for pumping the fluid is higher for the ducts having lesser duct angles.
- Triangular duct is consuming more pumping power compared to other geometric ducts.
- It is varying from 0.151 to 0.163 watts.
- Trapezoidal duct with 100 degrees is requiring less pumping power of 0.0615 to 0.666 watts for various Richardson numbers.

Contours of Different Ducts:

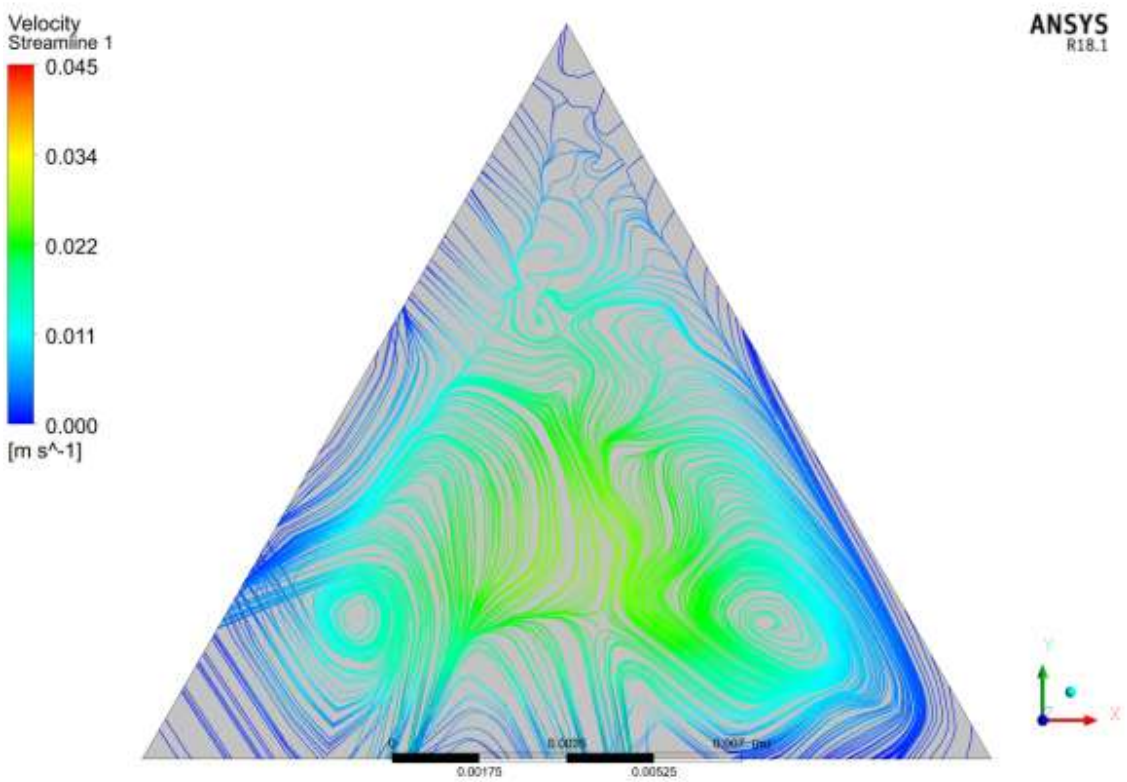

Figure-6: Equilateral Triangular duct

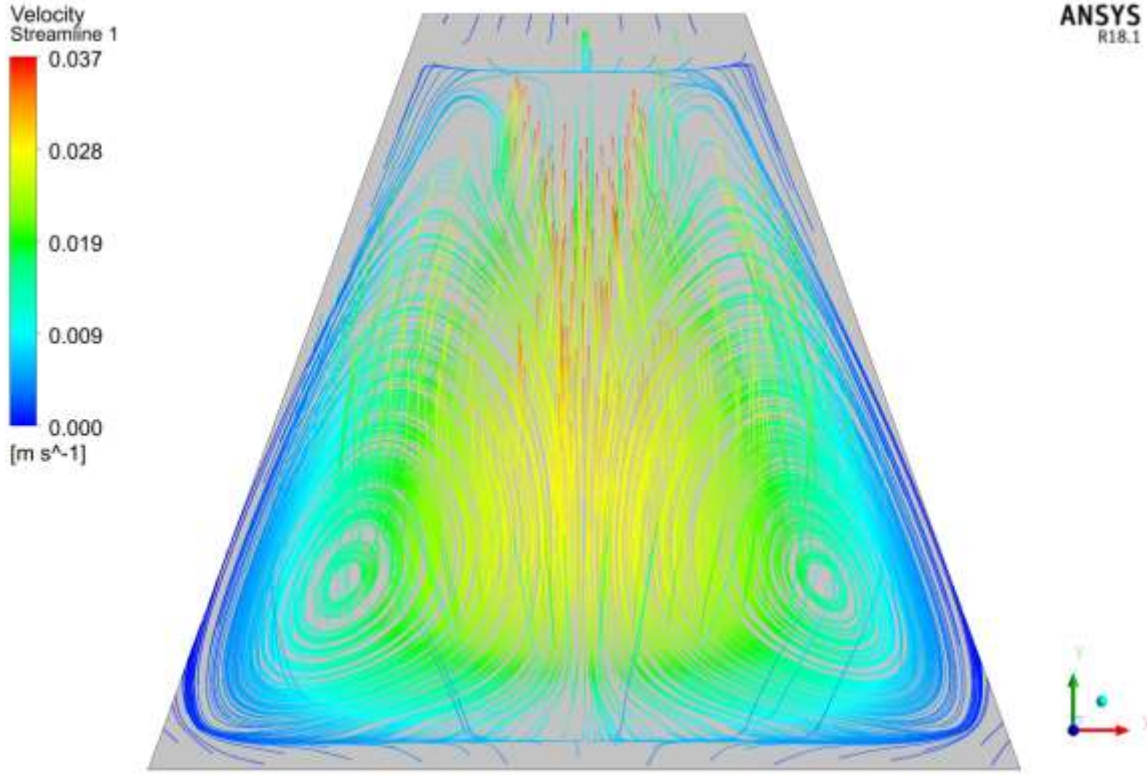

Figure-7:Trapezoidal duct of 70 degree angle

Contours of Different Ducts:

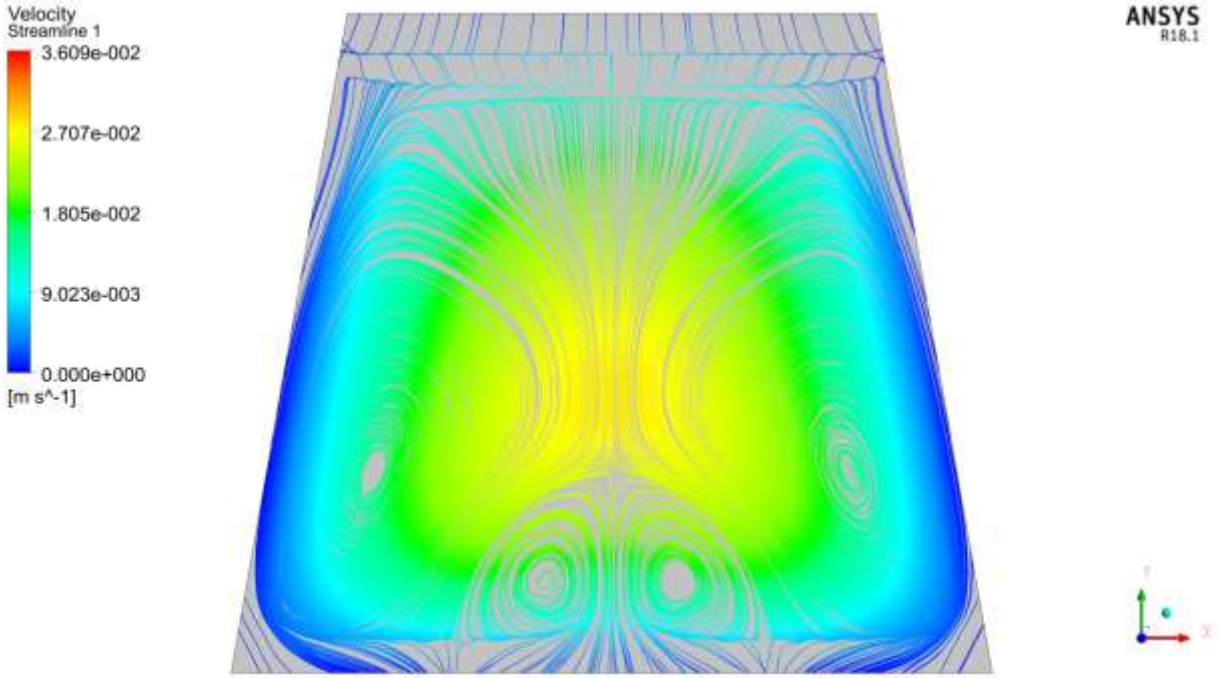

Figure-8: Trapezoidal duct of 80 degrees

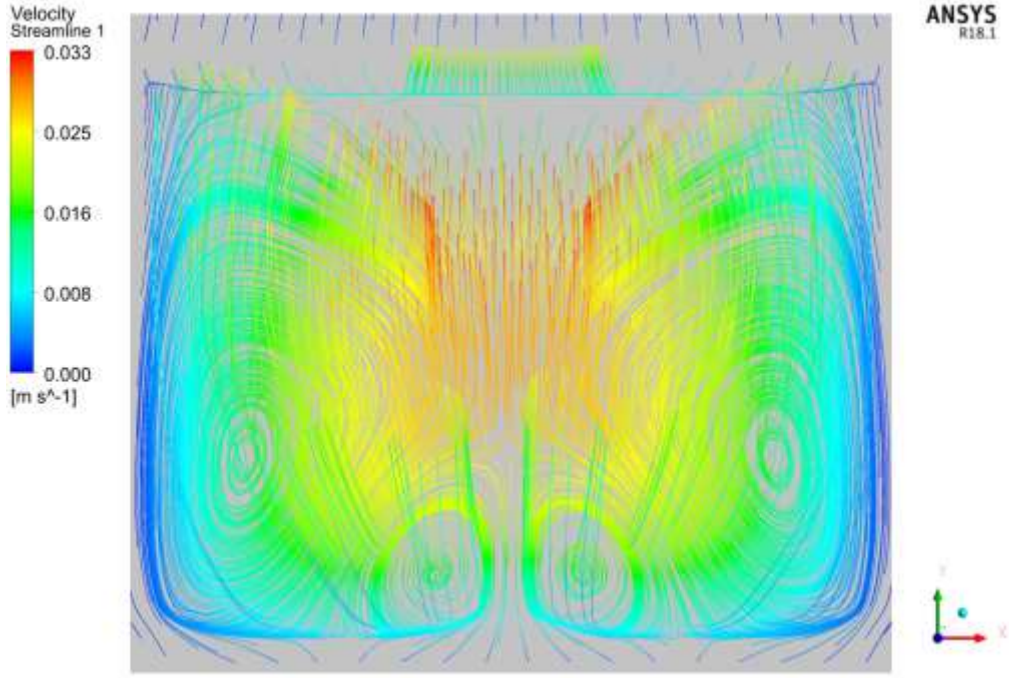

Figure-9: Trapezoidal duct of 90 degrees

Contours of Different Ducts:

- Here as angle of duct is increasing the no. of vortex formed in ducts are increasing.
- For triangle duct and duct with 70 degrees only two vortex are formed whereas for ducts with 80, 90, 100 degrees four vortex are formed.
- As number of vortex's increasing Heat Transfer coefficient and Nusselt Number values are increasing.
- More the number of vortex formed,more will be the mixing of fluids and more heat gets absorbed into fluid providing better convective heat transfer

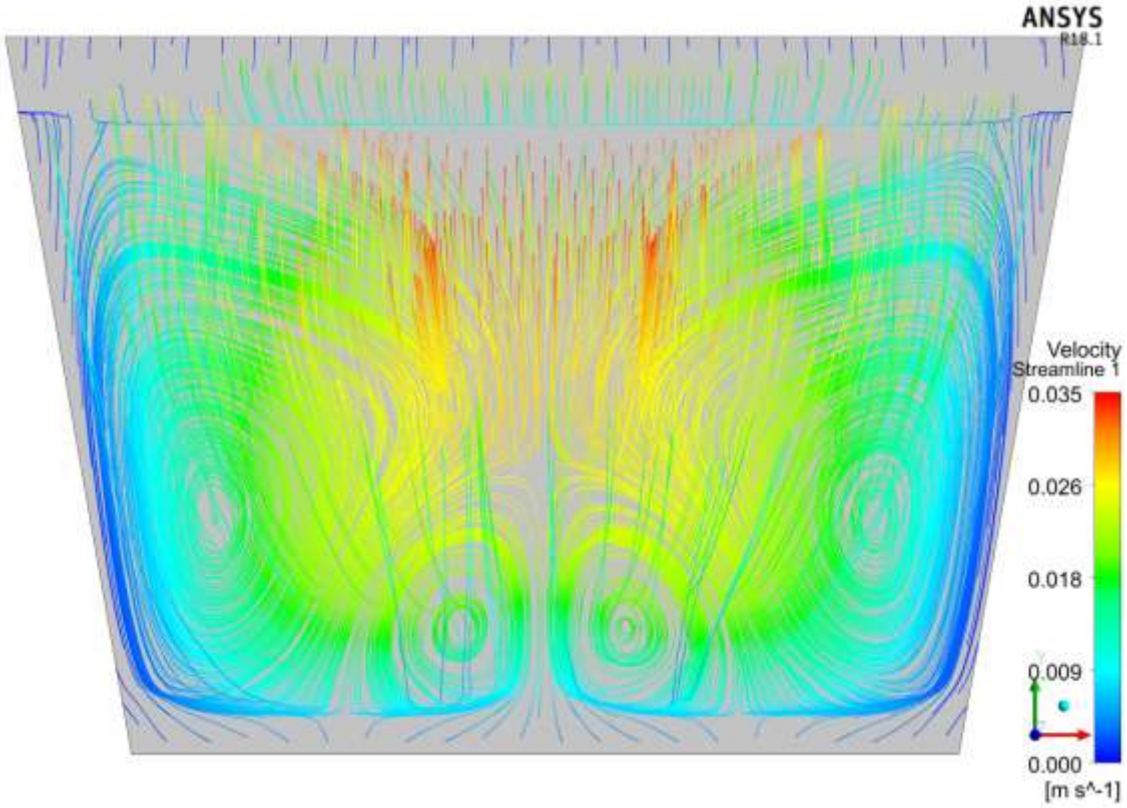

Figure-10: Trapezoidal duct of 100 degrees

Conclusions

- Water based Aluminum oxide nanofluid has higher heat transfer properties, it has greater Nusselt numbers and heat transfer coefficients. Also as Volume concentrations increasing properties are also getting improved with greater heat transfer.
- The only disadvantage of using Aluminum oxide-water based nanofluid is, it requires higher pumping power and also greater shear stresses are generated along the walls.
- Titanium oxide-water based nanofluid has better heat transfer capacity than the Silicon oxide-water based nanofluid.
- But silicon oxide-water based nanofluid requires lesser pumping power and having lesser shear stresses at lower concentrations.
- Trapezoidal ducts having more angle are having higher Nusselt Number and heat transfer coefficients.Whereas shear stress and pumping power are higher in lower angle Trapezoidal ducts.

Future Plans

- In further study we can improve the surface for better heat transfer. By increasing surface area there will be more heat conduction, this can be achieved by intrusion and protrusion of wall surface.
- Not only surface area we can also use various nanofluids like CuO-water, Silver oxide, Zinc oxide based nanofluids.

Nomenclature

A:	Cross-section area (m^2)
c_p:	Specific heat (J/kgK)
d:	Duct diameter (m)
f:	Friction factor
g:	Gravitational acceleration (m/s^2)
Gr:	Grashof number
h:	Heat transfer coefficient (W/m^2K)
H:	Duct height (m)
l:	Duct edge length (m)
L:	Total duct length (m)
Nu:	Nusselt number
P:	Pressure (Pa)
Pe:	Peclet number
PP:	Pumping power (W)
Pr:	Prandtl number(v/a)
q:	Heat flux (W/m^2)
Re:	Reynolds number
Ri:	Richardson number
T:	Temperature (K)
u, v, w:	Velocity component (m/s)
V:	Average velocity (m/s)
v:	Volume flow rate (m^3/s)
x, y, z:	Spatial coordinates (m).

Nomenclature

Greek Symbols:

α:	Thermal diffusivity (m^2/s)
β:	Volumetric expansion coefficient (1/K)
λ:	Thermal conductivity (W/m K)
μ:	Dynamic viscosity (Pa s)
ρ:	Density (kg/m^3)
τ:	Wall shear stress (kg/m)
v:	Kinematic viscosity (m^2/s)
π:	Nanoparticle volumetric concentration.

Subscripts:

avg:	Average
b_f:	Base fluid
f:	Fluid
h:	Hydraulic
m:	Mass
n_f:	Nanofluid
p:	Solid particle
w:	Wall.

References

[1] Aggarwala, B. D., & Gangal, M. K. (1975). Laminar flow development in triangular ducts. Transactions of the Canadian Society for Mechanical Engineering, 3(4), 231–233. https://doi.org/10.1139/tcsme-1975-0031

[2] Buongiorno, J., Venerus, D. C., Prabhat, N., McKrell, T., Townsend, J., Christianson, R., Tolmachev, Y. V., Keblinski, P., Hu, L.-W., Alvarado, J. L., Bang, I. C., Bishnoi, S. W., Bonetti, M., Botz, F., Cecere, A., Chang, Y., Chen, G., Chen, H., Chung, S. J., … Zhou, S.-Q. (2009). A benchmark study on the thermal conductivity of nanofluids. Journal of Applied Physics, 106(9), 094312. https://doi.org/10.1063/1.3245330

[3] Ferrouillat, S., Bontemps, A., Ribeiro, J.-P., Gruss, J.-A., & Soriano, O. (2011). Hydraulic and heat transfer study of SiO2/water nanofluids in horizontal tubes with imposed wall temperature boundary conditions. International Journal of Heat and Fluid Flow, 32(2), 424–439. https://doi.org/10.1016/j.ijheatfluidflow.2011.01.003

[4] Hanks, R. W., & Cope, R. C. (1970). Laminar-turbulent transitional flow phenomena in isosceles triangular cross-section ducts. AIChE Journal. American Institute of Chemical Engineers, 16(4), 528–535. https://doi.org/10.1002/aic.690160405

[5] Mohammed, H. A., Om, N. I., Shuaib, N. H., Hussein, A. K., & Saidur, R. (2011). The application of nanofluids on three dimensional mixed convection heat transfer in equilateral triangular duct. Heat and Technology, 29(2), 3–12. https://eprints.um.edu.my/6691/

[6] Montgomery, S. R., & Wibulsvas, P. (2019). Laminar flow heat-transfer in ducts of rectangular cross-section. Proceeding of International Heat Transfer Conference 3.

[7] Xuan, Y., & Li, Q. (2000). Heat transfer enhancement of nanofluids. International Journal of Heat and Fluid Flow, 21(1), 58–64. https://doi.org/10.1016/s0142-727x(99)00067-3

[8] Yilmaz, T., & Cihan, E. (1993). General equation for heat transfer for laminar flow in ducts of arbitrary cross-sections. International Journal of Heat and Mass Transfer, 36(13), 3265–3270. https://doi.org/10.1016/0017-9310(93)9000

[9] Zhou, S.-Q., & Ni, R. (2008). Measurement of the specific heat capacity of water-based Al2O3 nanofluid. Applied Physics Letters, 92(9), 093123. https://doi.org/10.1063/1.2890431.

[10] Talukdar P., Shah M., “Analysis of laminar mixed convective heat transfer in horizontal triangular ducts,” *Numerical Heat Transfer Part A: Applications*, vol. 54, no. 12, pp. 1148–1168, 2008.

[11] Lawal A., “Mixed convection heat transfer to power law fluids in arbitrary cross-sectional ducts,” *Journal of Heat Transfer*, vol. 111, no. 2, pp. 399–406, 1989.

[12] Schneider G. E., LeDain B. L., “Fully developed laminar heat transfer in triangular passages,” *Journal of energy*, vol. 5, no. 1, pp. 15–21, 1981.

[13] Hanks R. W., Cope R. C., “Laminar-Turbulent Transitional Flow Phenomena in Isosceles Triangular Cross-section Ducts,” *AIChE Journal*, vol. 16, no. 4, pp. 528–535, 1970.

[14] Altemani C. A. C., Sparrow E. M., “Turbulent heat transfer and fluid flow in an unsymmetrically heated triangular duct,” *Journal of Heat Transfer*, vol. 102, no. 4, pp. 590–597, 1980.

[15] Leung C. W., Wong T. T., and Kang H. J., “Forced convection of turbulent flow in triangular ducts with different angles and surface roughnesses,” *Heat and Mass Transfer*, vol. 34, no. 1, pp. 63–68, 1998. https://www.sciencedirect.com/science/article/abs/pii/S0142727X11000117

[16] Sharabi M., Ambrosini W., He S., and Jackson J. D., “Prediction of turbulent convective heat transfer to a fluid at supercritical pressure in square and triangular channels,” *Annals of Nuclear Energy*, vol. 35, no. 6, pp. 993–1005, 2008. .

[17] Chaves C. L., Quaresma J. N. N., Macˇdo N., Macědo E. N., Pereira L. M., and Lima J. A., “Forced convection heat transfer to power-law non-Newtonian fluids inside triangular ducts,” Heat Transfer Engineering, vol. 25, no. 7, pp. 23–33, 2004.

[18] Manca O., Nardini S., Ricci D., and Tamburrino S., “Numerical investigation on mixed convection in triangular cross-section ducts with nanofluids,” Advances in Mechanical Engineering, vol. 2012, Article ID 139370, 13 pages, 2012.

[19] Rehme K., “Simple method of predicting friction factors of turbulent flow in non-circular channels,” International Journal of Heat and Mass Transfer, vol. 16, no. 5, pp. 933–950, 1973.

[20] Lai Y. G., “An unstructured grid method for a pressure-based flow and heat transfer solver,” Numerical Heat Transfer, Part B: Fundamentals, vol. 32, no. 3, pp. 267–281, 1997.

[21] Chen S., Chan T. L., Leung C. W., and Yu B., “Numerical prediction of laminar forced convection in triangular ducts with unstructured triangular grid method,” Numerical Heat Transfer Part A: Applications, vol. 38, no. 2, pp. 209–224, 2000.

[22] Shah R. K., London A. L., Laminar Flow Forced Convection in Ducts, Academic Press, New York, NY, USA, 1978.

THANK YOU